ASTROBIOLOGY
Volume 10, Number 9, 2010

DOI: 10.1089/ast.2010.0513

Biogenicity of Morphologically Diverse Carbonaceous Microstructures from the *ca.* 3400 Ma Strelley Pool Formation, in the Pilbara Craton, Western Australia

Kenichiro Sugitani,[1] Kevin Lepot,[2] Tsutomu Nagaoka,[3] Koichi Mimura,[4] Martin Van Kranendonk,[5,6] Dorothy Z. Oehler,[6,7] and Malcolm R. Walter[6]

Abstract

Morphologically diverse structures that may constitute organic microfossils are reported from three remote and widely separated localities assigned to the *ca.* 3400 Ma Strelley Pool Formation in the Pilbara Craton, Western Australia. These localities include the Panorama, Warralong, and Goldsworthy greenstone belts. From the Panorama greenstone belt, large (>40 μm) lenticular to spindle-like structures, spheroidal structures, and mat-forming thread-like structures are found. Similar assemblages of carbonaceous structures have been identified from the Warralong and Goldsworthy greenstone belts, though these assemblages lack the thread-like structures but contain film-like structures.

All structures are syngenetic with their host sedimentary black chert, which is associated with stromatolites and evaporites. The host chert is considered to have been deposited in a shallow water environment. Rigorous assessment of biogenicity (considering composition, size range, abundance, taphonomic features, and spatial distributions) suggests that cluster-forming small (<15 μm) spheroids, lenticular to spindle-like structures, and film-like structures with small spheroids are probable microfossils. Thread-like structures are more likely fossilized fibrils of biofilm, rather than microfossils. The biogenicity of solitary large (>15 μm) spheroids and simple film-like structures is less certain.

Although further investigations are required to confirm the biogenicity of carbonaceous structures from the Strelley Pool Formation, this study presents evidence for the existence of morphologically complex and large microfossils at 3400 Ma in the Pilbara Craton, which can be correlated to the contemporaneous, possible microfossils reported from South Africa. Although there is still much to be learned, they should provide us with new insights into the early evolution of life and shallow water ecosystems. Key Words: Archean—Biogenicity—Microfossils—Pilbara. Astrobiology 10, 899–920.

1. Introduction

The *ca.* 3400 Ma Strelley Pool Formation (Hickman, 2008; formerly Strelley Pool Chert; Lowe, 1983) is a distinctive and widespread unit in the East Pilbara Terrane of the Pilbara Craton (Van Kranendonk *et al.*, 2004, 2006) (Fig. 1). This formation was deposited between 3426 and 3350 Ma and represents a shallow-water succession deposited under transitional subaerial to shallow submarine conditions (Lowe, 1983; DiMarco and Lowe, 1989; Allwood *et al.*, 2006; Van Kranendonk, 2006; Hickman, 2008). Areas of marine dolomite contain well-preserved and morphologically diverse stromatolites that are associated with evaporite minerals and carbonaceous black cherts (Lowe, 1980, 1983; Hofmann *et al.*, 1999; Van

[1]Department of Environmental Engineering and Architecture, Graduate School of Environmental Studies, Nagoya University, Nagoya, Japan.
[2]Department of Geology, University of Liège, Liège, Belgium.
[3]School of Informatics and Sciences, Nagoya University, Nagoya, Japan.
[4]Department of Earth and Environmental Sciences, Graduate School of Environmental Studies, Nagoya University, Nagoya, Japan.
[5]Geological Survey of Western Australia, Department of Mines and Petroleum, East Perth, Australia.
[6]Australian Centre for Astrobiology, University of New South Wales, Sydney, Australia.
[7]Astromaterials Research and Exploration Science, NASA Johnson Space Center, Houston, Texas, USA.

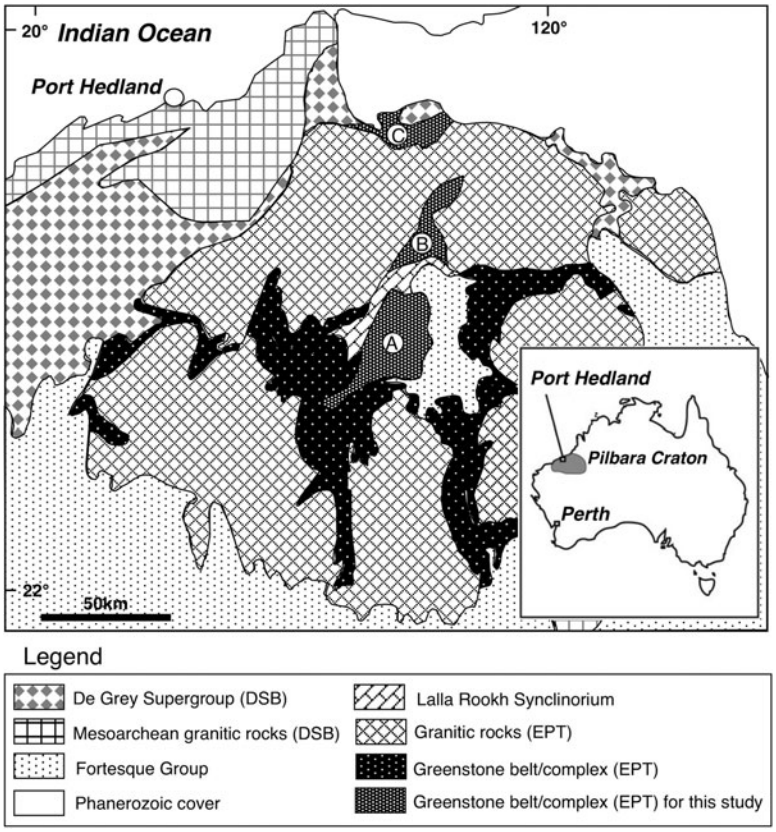

FIG. 1. Geology of northeastern part of the Pilbara Craton (after Hickman, 2008). DSB and EPT in the legend indicate De Grey Superbasin and East Pilbara Terrane, respectively. A, Panorama greenstone belt; B, Warralong greenstone belt; C, Goldsworthy greenstone belt.

Kranendonk *et al.,* 2003; Van Kranendonk, 2006). Their morphological diversity is likely controlled by environmental variation, as is the case for modern and younger equivalents (Allwood *et al.,* 2006, 2007; Van Kranendonk, 2007). Associated carbonaceous black cherts contain ^{13}C-depleted kerogen, which exhibits molecular profiles that suggest a biogenic origin (Marshall *et al.,* 2007; Van Kranendonk, 2007). These lines of evidence, together with other studies (*e.g.*, Allwood *et al.,* 2006; Van Kranendonk, 2007; Glikson *et al.,* 2008), suggest the presence of complex and diverse life at *ca.* 3400 Ma and the early evolution of shallow-water ecosystems.

On the other hand, there is skepticism regarding the biogenicity of stromatolites and kerogen in Archean black chert. For example, Lindsay *et al.* (2005) claimed that carbonaceous black chert of the Strelley Pool Formation (SPF) was of deep hydrothermal origin and ^{13}C-depleted organic matter was produced through abiogenic processes (McCollom and Seewald, 2006). Some studies have suggested the possibility of abiogenic formation of Archean stromatolites (Lowe, 1994; Grotzinger and Rothman, 1996; Grotzinger and Knoll, 1999; McLoughlin *et al.,* 2008; Wacey, 2009). Bona fide microfossils have not yet been reported from the SPF, although a few studies have suggested the possibility that some microstructures in this formation and the underlying Panorama Formation are biogenic (Brasier *et al.,* 2006; Westall *et al.,* 2006; Wacey, 2009).

In this paper, we describe carbonaceous structures from black cherts associated with stromatolites or evaporites, or both, at three remote and widely separated localities assigned to the *ca.* 3400 Ma SPF. Their biogenicity is discussed, following the same rationale as presented for the younger (*ca.* 3000 Ma) Farrell Quartzite microfossil assemblage from the Goldsworthy greenstone belt (*e.g.*, Sugitani *et al.,* 2007).

2. General Geology and Sampling Locations

The SPF is a widespread formation within the Pilbara Supergroup that has been identified in 11 greenstone belts of the East Pilbara Terrane (Van Kranendonk, 2006, 2007). The Pilbara Supergroup is composed of three groups and one formation, including the 3520–3427 Ma Warrawoona Group, the *ca.* 3400 Ma SPF, the 3350–3315 Ma Kelly Group, and the 3270–3235 Ma Sulphur Springs Group (Van Kranendonk *et al.,* 2007). These rocks are unconformably overlain by the 3200–3165 Ma Soanesville Group (Van Kranendonk *et al.,* 2010). The SPF was previously assigned to the Kelly Group (as the Strelley Pool Chert) but is now positioned independently between the Warrawoona and Kelly groups (Hickman, 2008).

The SPF is up to 1000 m in thickness and dominated locally by siliciclastic rocks (sandstone and conglomerate). However, a widespread characteristic feature of the formation is the presence of bedded dolomites, including stromatolitic laminates and layered gray-white cherts originating from silicified carbonates (chert laminite). As minor components, primary variegated (black-white-red) cherts and crystal pseudomorphs after carbonate, bicarbonate, and sulfate minerals have been identified (Lowe, 1983; Van Kranendonk *et al.,* 2004, 2006; Hickman, 2008). In many places, the depositional environment of the SPF has been interpreted as shallow-water marine, including tidal and supratidal environments. However, in some localities, evi-

dence of wider depositional environments, including fluviatile, lacustrine, and sabhka environments has been reported (Lowe, 1980, 1983; Allwood *et al.,* 2006; Van Kranendonk, 2007; Hickman, 2008).

For this study, we collected samples of black chert from the sedimentary successions assigned to the SPF in the Panorama greenstone belt, the Warralong greenstone belt, and the Goldsworthy greenstone belt (Fig. 1) in order to search for early life on Earth.

3. Methods and Terminology

3.1. Sample collection and handling

Rock specimens were collected in 2005 (the Panorama greenstone belt), 2007 (the Goldsworthy greenstone belt), and 2008 (the Warralong greenstone belt) by K.S. and K.M. The block samples, slabs, and thin sections are currently housed in the Nagoya University collection while studies are underway, but they will eventually be reposited in Australian collection, as required under the Australian Protection of Movable Cultural Heritage Act.

3.2. Microscopic analyses

Samples were cut into several slabs with a diamond saw, mostly perpendicular to bedding. Multiple petrographic thin sections (2.5×3.4 cm wide and $30 \sim 35$ μm thick) were made from each hand specimen (indicated by slide numbers with extensions, *e.g.,* WF4-1 and MSC1-3a). Microscopic examinations were carried out with a Leitz-DMRP with from $100\times$ to $1000\times$ magnification and a digital camera system (Leica DFC280). Positions of microstructures in thin section were recorded with an England Finder and are cited in the figure captions.

3.3. Organic geochemistry

3.3.1. Raman microspectroscopy. Raman spectra were obtained with a Renishaw InVia spectrometer (at Institut de Physique du Globe de Paris) with a 514.5 nm argon laser (20 mW; Spectra Physics) focused through an Olympus BX61 microscope with a $100\times$ objective (NA = 0.9). Raman spectra were recorded on carbonaceous particles located below the surface of polished thin sections to avoid artifacts that may be caused by the polishing process. The backscattered Raman signal was dispersed by a holographic grating and analyzed with a deep depletion CCD detector. Baseline subtraction was performed in Wire 3.2 by using a cubic spline interpolation with four fixed points (950, 1100, 1710, 1830 cm^{-1}).

3.3.2. Isolation and isotopic analyses of kerogen. Black chert samples were pulverized with a stainless steel mortar. Sample powders (150–350 g) were then treated with 6 *M* HCl to decompose carbonate. A mixed acid (HF:HCl = 4:1) was added to sample powders for digestion, followed by rinsing with distilled water. The residue was cleaned with hot HCl (80°C) for 48 hours, which yielded residues composed of kerogen and pyrite. Kerogen was separated from pyrite with use of a heavy liquid ($CHBr_3$; 2.9 g/cm^3) and was washed with $CHCl_2$ in soxhlet extraction apparatus for 72 hours.

The extracted kerogen (0.5–1.0 mg) was converted into CO_2 at 900°C for 4 hours, with CuO as an oxidizer in Vycor tubes. Carbon isotopic ratios, analyzed with dual-inlet isotope ratio mass spectrometry, are written in conventional δ-notations for the Pee Dee Belemnite (PDB) scale. The precision of the isotope ratio mass spectrometry analysis was ± 0.05‰.

3.4. Terminology of carbonaceous structures

To describe morphologies of carbonaceous structures, we employ the following terms in this study, including film-like, thread-like, spheroidal, lenticular, and spindle-like structures. These were first adapted to the Farrel Quartzite microfossil assemblage (Sugitani *et al.,* 2007). Detailed explanations for these terms are given below.

The term *film-like structure* describes a sheet-like object, including both single-sheeted and branching sheets, with or without attachment such as small spheroids. *Thread-like structure* describes a thin, nontubular filamentous object. The term *spheroidal structure* describes spherical to elliptical objects, including those with a single protrusion. Structures composed of a spherical to elliptical body with two spear-like protrusions that are parallel to the major axis of the body are designated as *spindle-like.* Some specimens that have an oval-shaped body are also involved. The term *lenticular structure* is adapted to a lens-shaped structure with acute edges and without apparent appendages. There are ambiguous and intermediate morphological types that cannot be classified into either lenticular or spindle-like structures. Thus, the broader term *lenticular to spindle-like structures* is used when describing lenticular and spindle-like structures, and such ambiguous specimens together.

It should be noted that these morphological terms are simply based on two-dimensional shapes of carbonaceous objects. For example, the body of spindle-like structures may be either prolate or oblate spheroid, whereas the spear-like appendages may be either cones attached at both ends of the body or a tapered flange surrounding the body (*e.g.,* Sugitani *et al.,* 2007, 2009a, 2009b). Variations in three-dimensional shape and other features are referred to individually, if necessary.

4. Panorama Greenstone Belt

4.1. Stratigraphy and sampling

In the Panorama greenstone belt (Fig. 1), the SPF *ca.* 30 m thick unconformably overlies the Panorama Formation and is overlain by the Euro Basalt (Van Kranendonk, 1999). Allwood *et al.* (2006, 2007) and Van Kranendonk (2007) performed detailed stratigraphic studies in this area and classified this formation into four members. These are, from base to top: a basal jasper/chert conglomerate (M1); laminated stromatolitic carbonate/chert (M2); bedded black chert with silicified evaporite beds, and silicified pebble conglomerate and stromatolitic laminated ironstone (M3); and silicified, fining-upward clastic/volcaniclastic rocks cut by hydrothermal vein chert (M4). M1 is interpreted to have been deposited on a rocky shoreline, whereas M2 was deposited in an isolated peritidal carbonate platform, and M3 in possible shallow restricted conditions. M4 probably represents a deepening upward succession deposited in subsiding fault blocks, during onset of hydrothermal activity (Allwood *et al.,* 2006, 2007; Van Kranendonk, 2007).

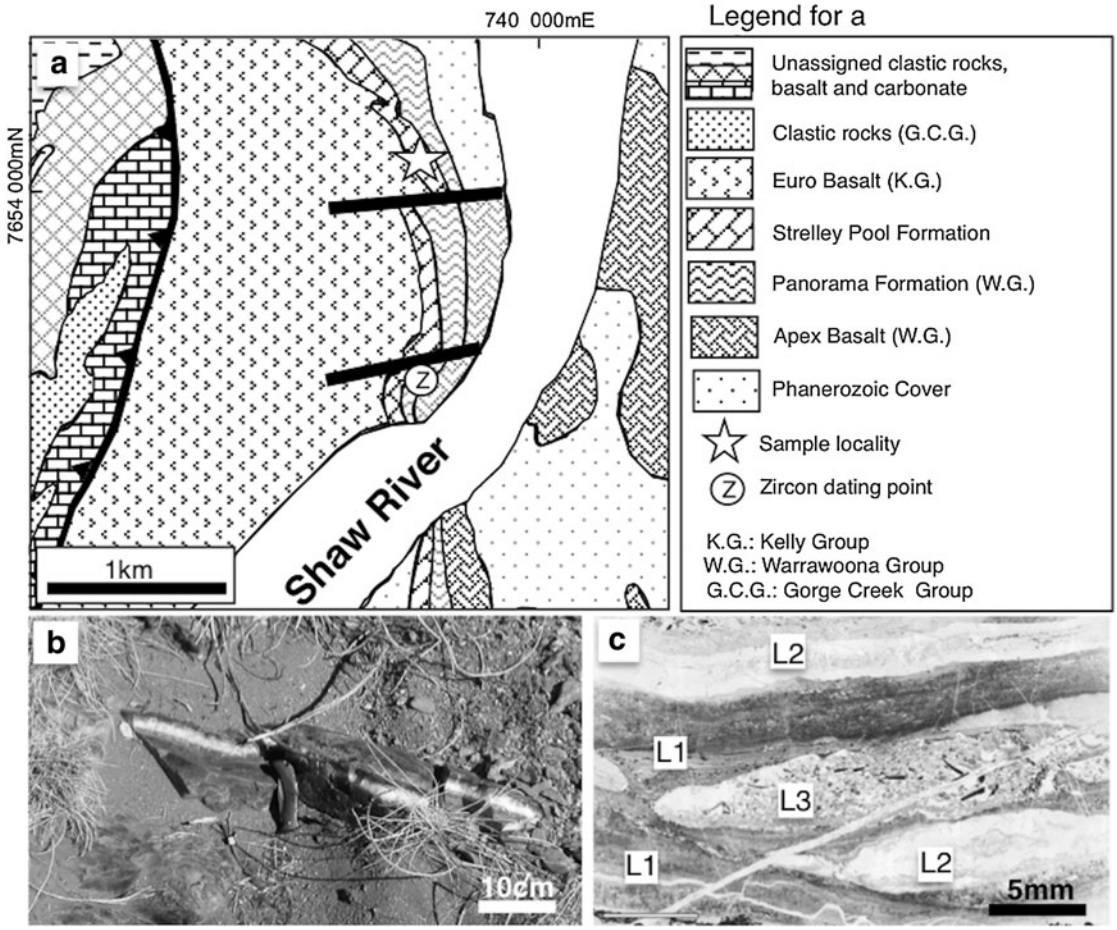

FIG. 2. (**a**) Local geology of the Anchor Ridge site (the Panorama greenstone belt) (after Van Kranendonk, 1999). Thick line shows fault. (**b**) Photograph of black chert layer from which samples were collected. A knife 10 cm long for scale. (**c**) Photomicrograph of banded black chert. Scale bar: 5 mm. L1, carbonaceous layer; L2, secondary cavity-fill chert; L3, detrital layer.

Samples were collected from the south bank of an unnamed creek that cuts through the SPF along the Shaw River (21°11′46″S, 119°18′23″E, hereafter designated as Anchor Ridge site; Fig. 2a). At this locality, a few meters of bedded black cherts contain thin, discontinuous cavity-fill white chert (Fig. 2b). Van Kranendonk (2007) described wind-generated ripples from this unit along strike, indicative of very shallow water conditions. The bedded black chert is correlated to M3. Two black chert samples (TRD1 and TRD2) were collected, and fossil-like carbonaceous objects from TRD2 are described below.

4.2. Petrography of black chert

Although the black chert appears massive in hand specimen, thin layers of three distinct petrographic types were identified under the microscope. They are designated here as carbonaceous chert (L1), cavity fill chert (L2), and detrital layer (L3), respectively (Fig. 2c). The carbonaceous chert layer (L1) is enriched in carbonaceous particles, with minor sulfide, carbonate, and silicified prismatic minerals (probably barite). In most portions, this layer displays a complex network pattern, with spheroidal masses composed of microcrystalline quartz (Fig. 3a). The network pattern often horizontally and laterally merges into mat-like lamination (Fig. 3b). Locally, a thin layer that does not display either a network pattern or mat-like lamination is present. These layers are enriched in minute sulfide particles and aggregates. Carbonaceous particles are homogeneously distributed in some places of the matrix, whereas other areas comprise fine lamination or a heterogeneous distribution pattern (Fig. 3e, 3f). Cavity-fill chert L2 occurs as lenses and layers. The margins are composed of microcrystalline quartz, which shows chalcedonic extinction, whereas the central portion tends to be filled with mega-quartz, a mosaic of kaolinite and barite (Fig. 2c). Detrital layer L3 contains variously shaped, medium- to very coarse–grained clasts of carbonaceous chert, noncarbonaceous chert and aggregates of sulfides, and silicified barite crystals (Fig. 2c).

4.3. Occurrence of carbonaceous structures

Fossil-like carbonaceous structures were identified only in the L1 layer. Thin thread-like structures can be seen locally in portions that display a network pattern. Broad carbonaceous objects without a clear outline comprise most portions (Fig. 3a). The threads are less than 0.5 μm in diameter and entangled and possibly branched, with minute carbonaceous

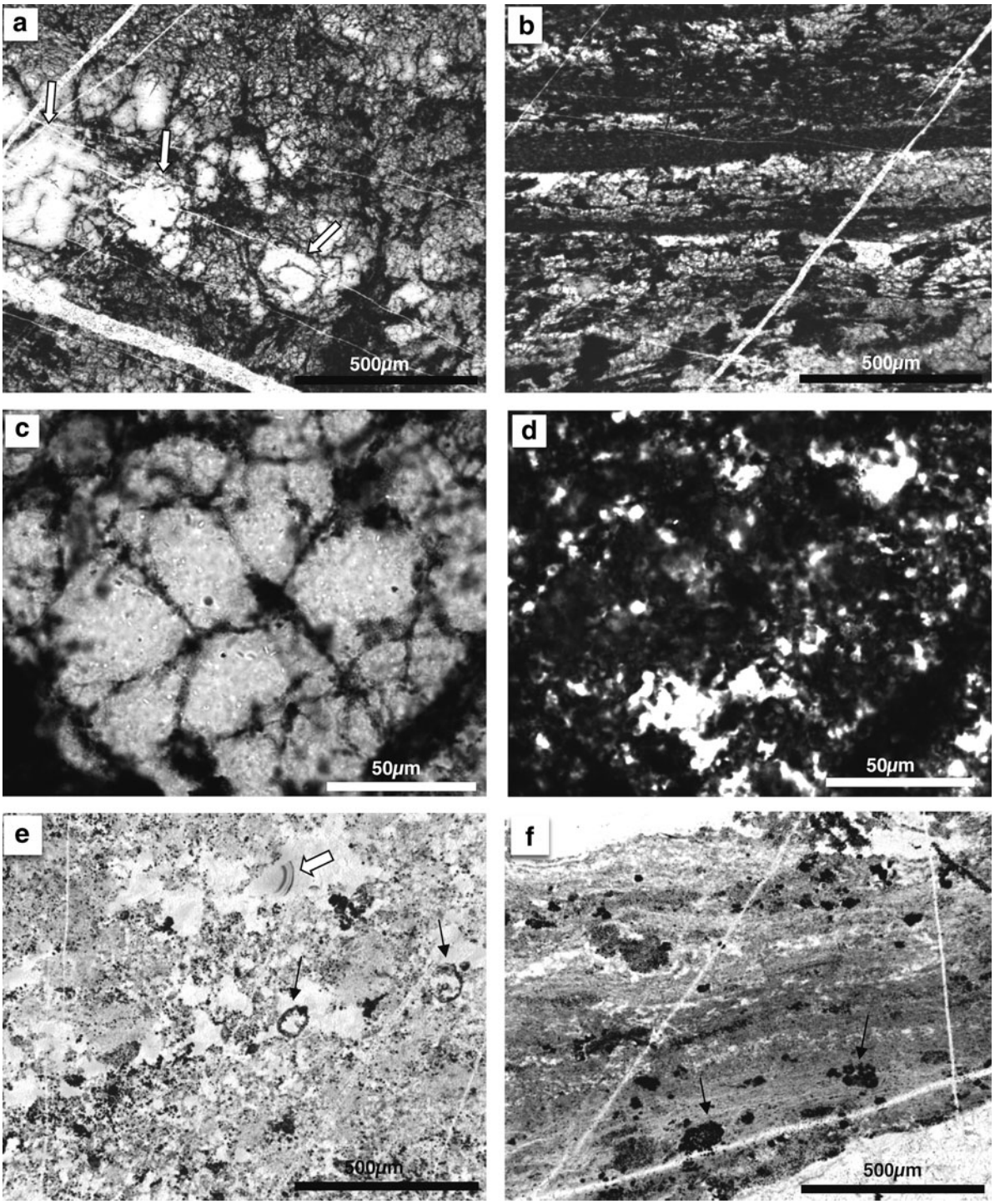

FIG. 3. Photomicrographs of carbonaceous layer (L1) of banded black chert from the Anchor Ridge site. (**a**) Carbonaceous layer showing a network pattern, with local spheroidal textures (arrows). (**b**) Parallel laminated carbonaceous layer transitional to portion characterized by a network pattern. (**c**) Enlarged spheroid-ovoid textures in which thin carbonaceous threads can be identified within nearly pure chert, under transmitted light. (**d**) The same portion as (c) under polarized light. Morphology and distribution patterns of carbonaceous threads are independent of the crystal boundaries of matrix microquartz mosaic. (**e**) Relatively massive portion of carbonaceous layer with abundant minute pyrite particles and irregularly shaped pure chert masses. The thin arrows show carbonaceous spheroids. The left one is a specimen shown in Fig. 4c. The thick white arrow shows colloform texture identified by carbonaceous particles, suggesting redistribution of organic matter. (**f**) Weakly laminated pyrite-rich carbonaceous layer. The arrows show pyrite aggregates.

clots (Fig. 3c). Their shapes and distribution pattern are independent of the matrix quartz crystals (Fig. 3d).

In the pyrite-rich portions, spheroidal and lenticular to spindle-like carbonaceous structures are present. Within one thin section (TRD2a-3), 10 specimens of solitary spheroids were identified. Solitary carbonaceous spheroids range from 23 to 106 μm in average diameter and are mostly hollow. Walls are granular in most samples, and thus their textures are unclear (Fig. 4a), whereas, in a few samples, hyaline walls appear to be preserved. They are wrinkled or folded, or both, to various degrees (Fig. 4b, 4c). The inner portions of hollow spheroids are filled with microcrystalline quartz, and their wall outlines are independent of matrix crystal boundaries. In addition to solitary occurrences, spheroidal objects from 10 to 30 μm in diameter are found to comprise colony-like clusters, although shapes of individual objects are not always clear.

Thirty-eight lenticular to spindle-like structures were identified in a single thin section (TRD2a-3). Spindle-like structures dominate the population (30 individual examples), and there are eight lenticular structures. The size of these structures ranges from 35 to 119 μm along the major dimension. Some specimens occur as pairs or as clusters composed of less than five individuals (Fig. 4e). Most of the spindle-like structures have elliptical and hollow body shapes, with some specimens having an oval-shaped body, some a granular semi-hollow one, others a combination of the two (Fig. 4e–h). Whereas the wall of the body is generally

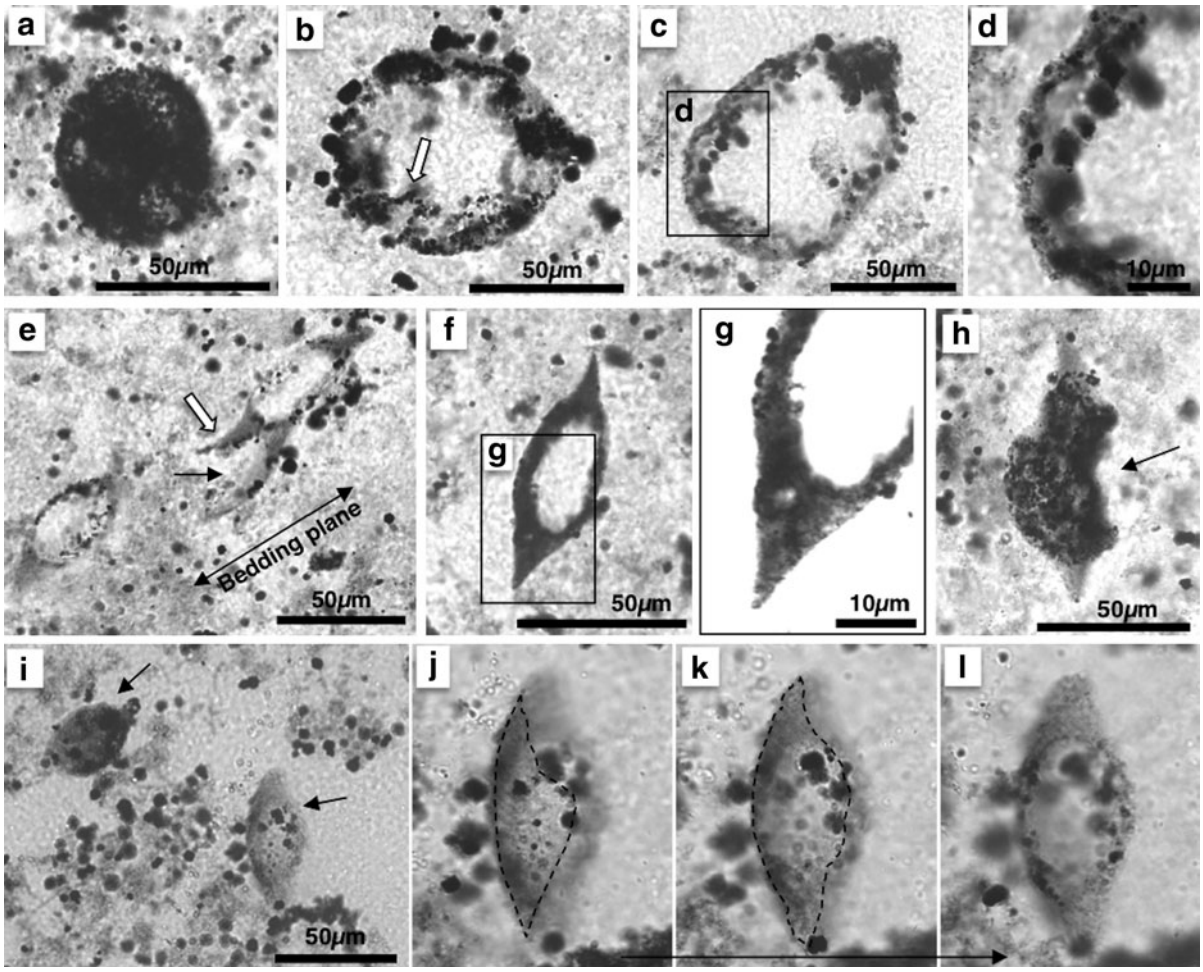

FIG. 4. Photomicrographs of carbonaceous structures in pyrite-rich carbonaceous layer (L1) of the Anchor Ridge black chert. All specimens are from a single thin section (TRD2a-3). (**a**) Granular walled spheroid. Position: L-C44/3. (**b**) Slightly deformed granular walled spheroid, with attached tiny pyrite cubes. The arrow shows the wrinkled portion of the wall. Position: L-Y56/4. (**c**) Distorted spheroid. Pyrite cubes and globules are attached with wall. Position: L-L63. (**d**) Magnification of (c). Weakly folded wall is less granular compared with the specimens in (a) and (b). (**e**) Three hollow spindle-like structures nearly parallel aligned. Note that the central specimen (the thin arrow) is sectioned. The appendage of the upper specimen is slightly curved (the white arrow). Position: L-D64/2. (**f**) Thick-walled hollow spindle, nearly perpendicular to the bedding plane, parallel to the horizontal line of the photograph. Position: L-F64/3. (**g**) Magnification of (f) under intense transmitted light, indicating that the wall and the appendage are translucent and heterogeneous. (**h**) Spindle-like structure having granular body and homogeneous appendage. Note that the body appears to be partially broken (the arrow). Position: L-D61/4. (**i**) Two lenticular structures (arrows), one of which has clearly identifiable flange-like appendage (see j–l). Position: L-L63. (**j–l**) Magnifications of the right specimen in (i) under the three different focal depths. The arrow shows the deepening focal depth. The dashed lines in j and k show the on-focus outline.

granular or blurred (probably due to alteration), some specimens have relatively thick and clearly identifiable walls (Fig. 4f). Deformed or broken bodies can also be seen (Fig. 4h). In many of the hollow spindle-like structures, their spear-like appendages are composed of the same material as the body and appear to be structurally continuous with the bodies. Specimens with a semi-hollow and highly granular body tend to have appendages composed of homogeneously distributed, very fine carbonaceous particles (Fig. 4h). The lengths of the two appendages of any given spindles are not always the same. Curved appendages are also present (Fig. 4e). These appendages, in most cases, surround the elliptical body like a flange (Fig. 4i–l) and are tapering; thus, they appear to be spear-like in a two-dimensional view.

5. Warralong Greenstone Belt

5.1. Stratigraphy and sampling

In the Warralong greenstone belt (Fig. 1), the SPF is composed dominantly of quartz-rich sandstone (Van Kranendonk, 2004b). At the sampling site near the Marble Bar Road (hereafter called the Marble Bar Road site) (Fig. 5a), the thickness of the SPF is >200 m (Van Kranendonk, 2004b; Hickman, 2008). Detrital zircons from this sandstone give a maximum depositional age of 3426 ± 10 Ma (Nelson, 1998).

The quartz-rich sandstone is conformably overlain by a cherty unit, *ca.* 10 m thick (Fig. 5b, 5d). This unit is composed mostly of white–light gray–black laminated chert, which is most likely silicified carbonate, with intercalated sandstone and white–light gray massive chert (Fig. 5e). The massive chert has vertically to subvertically oriented giant crystal pseudomorphs, which implies that it was originally an evaporite crystal set. This massive chert occurs at two horizons. Its thickness is laterally uneven, particularly at the upper horizon, where the massive chert appears to be locally scoured and filled by clastic material (Fig. 5c, 5f). This complex subunit is overlain by laminated to banded gray-black chert, locally with possible stromatolitic structures. This evaporite-clastic-chert unit is unconformably overlain by a *ca.* 2 m thick chert pebble conglomerate (Fig. 5g).

Three samples (MSC1-1 ~ 3) were collected from the laminated to banded gray-black chert, two (MSC1-1 and MSC1-2) from the outcrop where the stratigraphic section was measured (20°49′45.20″S, 119°30′02.50″E), and another (MSC1-3) from the same horizon along strike 50 m to the south.

5.2. Petrography of black chert

Sample MSC1-1 is massive and gray in color, with thin black or translucent white chert layers. The gray portion is enriched in irregularly shaped detrital lithic grains, with a trace amount of detrital quartz grains (upper half of Fig. 6a). The lithic grains are composed dominantly of microcrystalline quartz, with gray to brown particles of unknown origin and, in some cases, trace amounts of sericite. The black chert layer is *ca.* 1 cm thick. It is finely laminated and enriched in carbonaceous matter (the lower half of Fig. 6a). It contains abundant prismatic crystal ghosts, possibly silicified gypsum (Fig. 6b). Sample MSC1-2 is predominantly composed of layers or lenses of mega-quartz or microcrystalline quartz masses, with minor carbonaceous laminae. Fossil-like carbonaceous objects were identified in such carbonaceous laminae, which are heterogeneously silicified and characterized by abundant irregularly shaped pure chert masses (Fig. 6c). Parallel-laminated MSC1-3 is carbonaceous and contains abundant sulfide particles. This sample is heterogeneously silicified or ferruginized. The carbonaceous portions of this sample, in which fossil-like carbonaceous objects were observed, are texturally similar to the carbonaceous layer of MSC1-2.

5.3. Occurrence of carbonaceous structures

Three types of carbonaceous structures were identified in six analyzed thin sections, including film-like, spheroidal, and lenticular to spindle-like structures, (MSC1-1a, MSC1-2a, MSC1-2b, MSC1-2c, MSC1-3a, and MSC1-3b). MSC1-1a yields only a few film-like structures. The MSC1-2 series of sections contains 14 specimens, including films, spheroids, and lenticular to spindle-like structures. The MSC1-3 series thin sections contains a prolific assemblage of carbonaceous structures. Two clusters of spheroids and 55 lenticular to spindle-like structures were identified from duplicated thin sections (MSC1-3a, MSC1-3b).

Film-like structures range up to 200 μm along the major dimension (Fig. 7a–c). They are wrinkled or folded, or both, to various degrees. The surface of these structures is granular and locally has attached carbonaceous clots or sulfide grains (Fig. 7a). Spheroidal structures range from *ca.* 5 μm to 54 μm in diameter. They occur solitarily or as clusters composed of more than 10 small individuals (Fig. 7d), although the exact number of composite spheroids is uncertain due to the presence of ambiguous objects. The walls of the spheroids are preserved to various degrees: some specimens have hyaline walls; others have only the trace of a wall (Fig. 7e, 7f). The dominant wall type is granular. One spheroid specimen up to 54 μm in diameter (Fig. 7g) is hollow and has a partially broken wrinkled wall (Fig. 7h).

Spindle-like structures range from 44 to 120 μm along the major dimension, whereas lenticular structures are from 47 to 94 μm. These structures generally occur solitarily (Fig. 7i) and rarely comprise a parallel aligned or a randomly oriented cluster (Fig. 7j). One dumbbell-like object composed of linearly connected spindles was found (Fig. 7k). Spindle-like structures tend to have elliptical bodies, many of which are hollow (Fig. 7j–l), although some are semi-hollow and highly granular. The walls of spindle-shaped bodies are generally granular, rarely partially broken, and contain carbonaceous clots (Fig. 7l). Spear-like appendages of the spindle-like structures are, in most cases, composed of homogeneously distributed, fine carbonaceous particles and are structurally continuous with the body; one specimen has a large clot in the appendage (Fig. 7j). The lengths of two appendages of any given spindle are often not identical with each other, and curved appendages are present. As is the case for the Anchor Ridge spindles, the appendages are in many cases actually a flange that surrounds the elliptical body (Fig. 7m, 7n).

6. Goldsworthy Greenstone Belt

6.1. Stratigraphy and sampling

In the Goldsworthy greenstone belt (Fig. 1), the sedimentary successions assigned to the Strelley Pool Chert and the

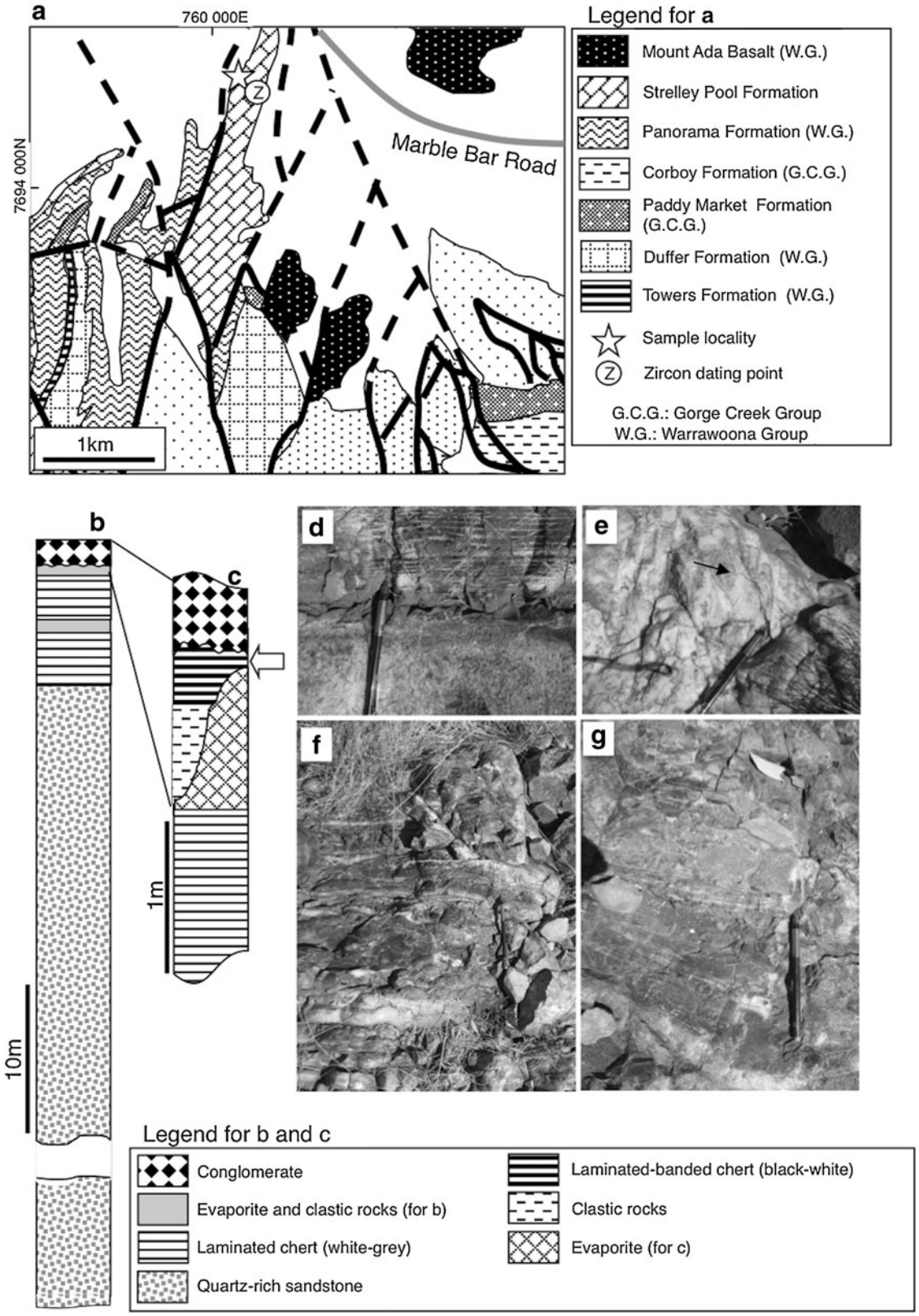

FIG. 5. (**a**) Local geology of the Marble Bar Road site (the Warralong greenstone belt) (after Van Kranendonk, 2004a, 2004b). Thick lines and dashed lines show faults and estimated faults, respectively. (**b** and **c**) Schematic stratigraphic columns at the sampling site. The white arrow in (c) indicates the sampling horizon. (**d**) Quartz-rich sandstone and conformably overlying laminated chert. (**e**) Massive white chert containing crystal pseudomorphs (the arrow), probably silicified evaporite. (**f**) Photograph of the uppermost chert section. (**g**) Closer view of bedded black chert containing fossil-like structures and overlying conglomerate. A pen 15 cm long for scale in (d–g).

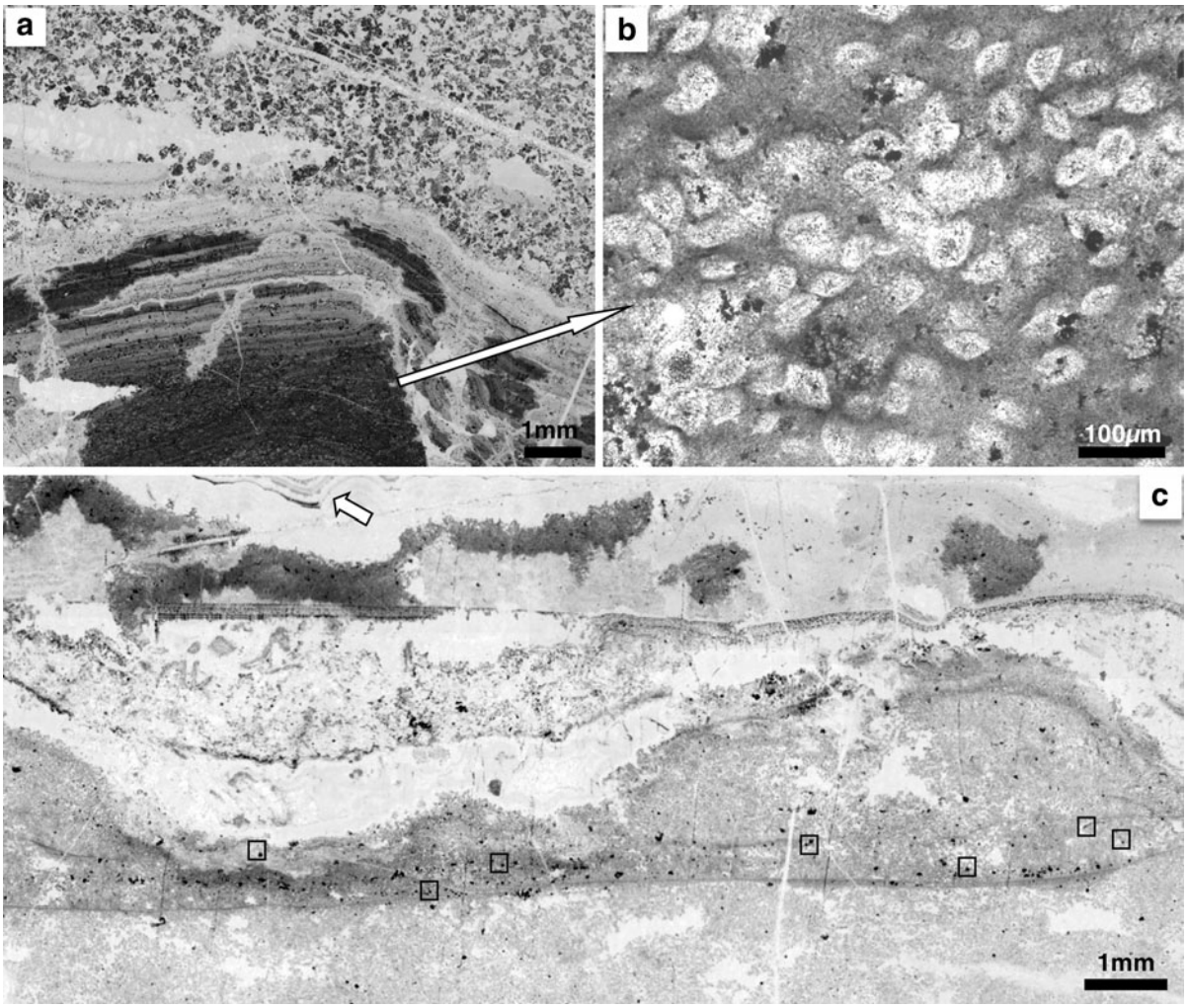

FIG. 6. Photomicrographs of bedded black chert containing fossil-like structures from the Marble Bar Road site. (**a**) A dark thin layer enriched in carbonaceous matter in the matrix composed of detrital grains (dark gray chert) (Sample MSC1-1a). (**b**) Spindle- to rhombic-shaped crystal ghosts, possibly derived from gypsum in a dark layer of the specimen in (a). Note that these structures lack carbonaceous wall. (**c**) Heterogeneously silicified bedded black chert containing fossil-like structures (squares) (MSC1-2a). Fine lamination can be locally identified. The arrow shows the portion showing colloform texture in which carbonaceous particles are concentrated.

Panorama Formation were mapped across the western part of Mount Grant and within an unnamed ridge to the north of Mount Grant (Smithies *et al.*, 2004). Hickman (2008) implied that the whole succession formerly assigned to the Strelley Pool Chert and the Panorama Formation in this area could represent the SPF. The sampling site (20°20′39″S, 119°25′09″E) is located at this unnamed ridge, which is hereafter informally called the Water Fall Ridge (Fig. 8a).

At the Water Fall Ridge site, the sedimentary succession is dominated by quartz-rich sandstone up to 100 m thick, with five interbedded cherty units 1.5–3 m in thickness (Fig. 8b). The lower three cherty units are finely laminated and white to light gray in color, interpreted to represent silicified carbonate rocks (chert laminite). Silicified evaporite is present as massive chert with silicified prismatic crystals in the two of the cherty units. The uppermost chert unit is distinct from the others by containing two stromatolitic horizons, which are interbedded with beds of massive black chert, laminated to banded white-black chert, chert breccia, and conglomerate-sandstone (Fig. 8c–g). The true original thickness of the succession at this locality is unknown, as the upper contact is an unconformity overlain by mafic to ultramafic volcaniclastic rocks of the Euro Basalt (Fig. 8f). Three chert samples (WF4, WF6, WF9) collected from this uppermost unit were examined. Sample WF4 is from a massive black chert overlying stromatolitic chert, whereas samples WF6 and WF9 were collected from laminated to banded black-white chert and a chert breccia set in a sandstone matrix (Fig. 8c, 8g).

6.2. Petrography of black chert

The massive black chert layer overlying the upper stromatolitic chert (WF4) (Fig. 8c, 8f) is carbonaceous and has irregularly shaped pure chert masses (Fig. 9a). Sulfide particles and aggregates are present. The chert is partially brecciated. Interstices between chert clasts are filled with mica, oxide particles (TiO_2 and Fe_2O_3), angular pure cherts, and monocrystalline quartz. Samples WF6 and WF9 of

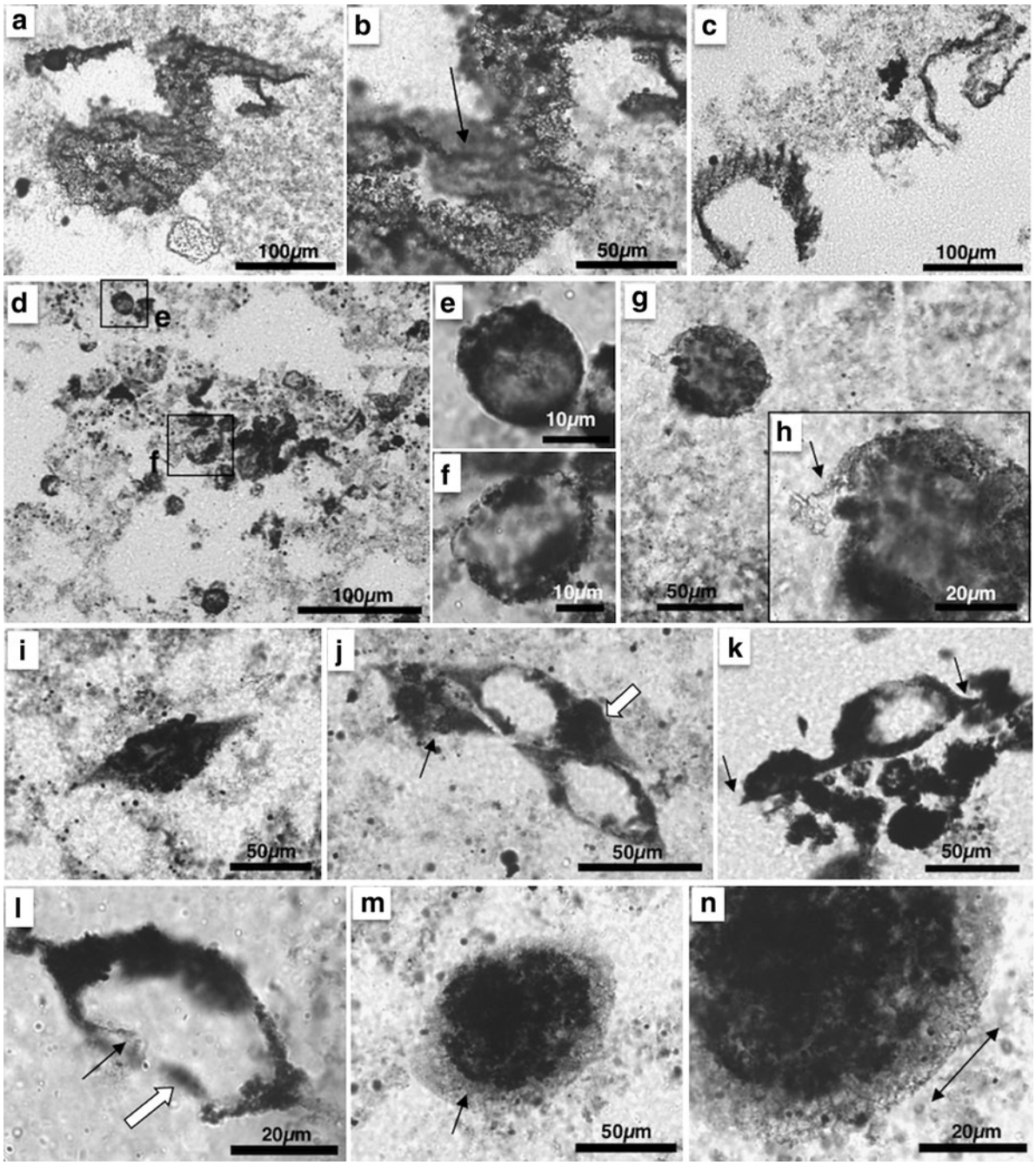

FIG. 7. Photomicrographs of carbonaceous structures from the Marble Bar Road site. (**a**) Film-like structure. Slide MSC1-2a, Position L-M60. (**b**) Magnification of (a). The film-like structure is granular. The arrow indicates the portion out of focus, indicating the folded shape of this structure. (**c**) Two film-like structures showing different degrees of folding. Slide MSC1-2a, Position L-R47. (**d**) Loose colony-like cluster of small spheroids. Slide MSC1-3b, Position L-Z57/4. (**e**, **f**) Magnifications of two spheroids in (d) showing different preservation status. Specimen in (e) appears to have hyaline wall, whereas specimen in (f) is poorly preserved. (**g**) Solitary large hollow spheroid. Slide MSC1-2c, Position L-P64/2. (**h**) Magnification of (g). Wall is partially broken (the arrow). (**i**) Spindle-like structure showing an asymmetrical attachment of flange (an equatorial view). Slide MSC1-3c, Position L-E59/4. (**j**) Three spindle-like structures parallel and tightly aligned. The thin arrow indicates the smallest one. The white arrow shows a large carbonaceous clot in the appendage. Slide MSC1-3b, Position L-W58/1. (**k**) Dumbbell-like structure composed of linearly connected spindles. The arrows indicate spear-like appendages. Note one of spindles is hollow, whereas the other appears to not be hollow. Slide MSC1-3c, Position L-D64. (**l**) Hollow lenticular structure, with partially broken wall (the white arrow). The thin solid arrow indicates folding of the wall. Slide MSC1-3b, Position L-Z56/4. (**m**) A polar view of inclined spindle-like structure with a flange-like appendage (the arrow) surrounding the body. Slide MSC1-3b, Position L-V67/1. (**n**) Magnification of (m). The double-arrowed bar indicates the portion of the appendage in focus. The other portions are out of focus, indicating that the appendage is shaped like a flange.

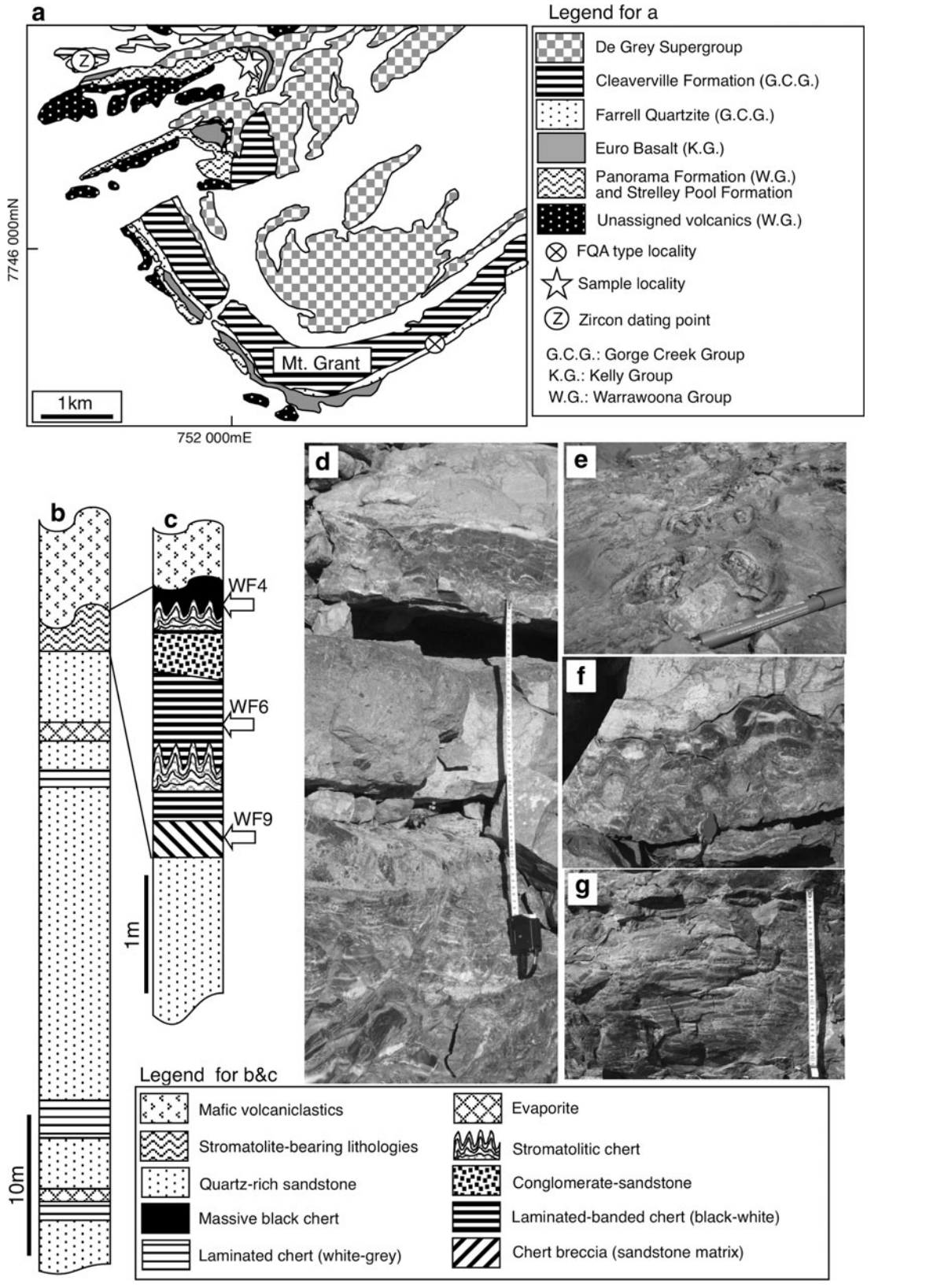

FIG. 8. (**a**) Local geology of the western part of the Goldsworthy greenstone belt (after Smithies *et al.,* 2004) and the sampling site. FQA type locality in "Legend for a" indicates the site from which the *ca.* 3000 Ma Farrel Quartzite microfossil assemblage was described (*e.g.,* Sugitani *et al.,* 2007). (**b**, **c**) Schematic stratigraphic columns. The arrows show the sampling horizons. (**d**) An overview of the cherty unit. The measure length is *ca.* 50 cm. (**e**) Horizontal view of stromatolitic chert. A pen 15 cm long for scale. (**f**) A closer view of the uppermost massive chert and unconformably overlying mafic volcaniclastic unit. (**g**) Tabular chert breccia in sandstone. The measure length is 30 cm.

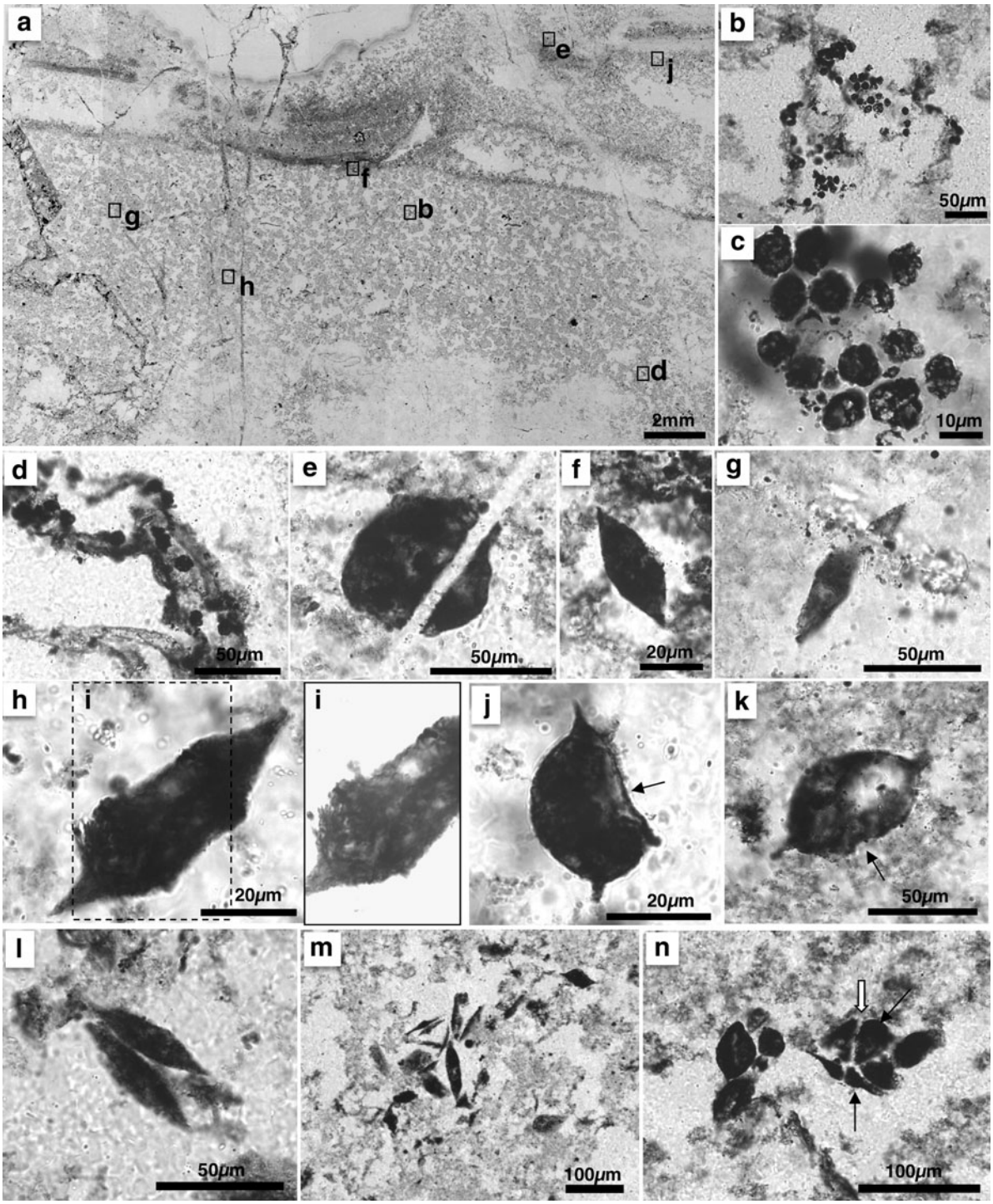

FIG. 9. Photomicrographs of massive black chert from the Water Fall Ridge site and carbonaceous structures. (**a**) Composite photomicrographs of heterogeneously silicified, massive black chert with abundant irregularly shaped pure chert masses (WF4-1). The squares show the positions of structures shown in this figure. (**b**) Cluster of small spheroids associated with film-like structure. Slide WF4-1, Position L-S52/2. (**c**) Magnification of (b). (**d**) Relatively hyaline wrinkled film-like structure with carbonaceous spherules. Slide WF4-1, Position L-M43/2. (**e**) Large spheroid having heterogeneous inner texture. This specimen is cut by vein quartz. Slide WF4-1, Position L-Y47/4. (**f**) Lenticular structure solid in appearance. Slide WF4-1, Position L-T54/2. (**g**) Hollow lenticular structure, with a hyaline wall. This specimen is cut by vein. Slide WF4-1, L-R63. (**h**) Spindle-like structure nearly solid in appearance. Slide WF4-1, Position L-P59. (**i**) The same specimen as (h) under the intense transmitted light, revealing its translucent and heterogeneous interior. (**j**) Spindle-like structure having deformed hyaline wall (the arrow). Inner portion is mostly filled with opaque objects, but partially hollow. Slide WF4-1, Position L-V51. (**k**) Hollow spindle with partially deformed wall (the arrow). Slide WF4-5, Position L-W56/1. (**l**) Obliquely arranged, paired lenticular structures. Slide WF4-5, Position L-L56/2. (**m**) Colony-like cluster of lenticular structures. Slide WF4-7, Position L-J48/4. (**n**) Colony-like cluster of lenticular to spindle-like structures. The thin solid arrows show specimens cut by a common vein (the white arrow).

laminated to banded chert are composed of alternations of black and white chert laminae from 1 mm to 1 cm in thickness (Fig. 10a). Black carbonaceous laminae are enriched in minute particles of sulfide. Carbonaceous matter occurs as cloudy material and particles. Most of white laminae are exclusively composed of mega-quartz crystals, microcrystalline quartz masses, or both.

6.3. Occurrence of carbonaceous structures

Four major types of carbonaceous structures were present in three analyzed thin sections from this locality, including film-like, spheroidal, lenticular, and spindle-like structures (WF4-1, WF6-1, and WF9-1). WF4-1 is prolific, with 148 lenticular to spindle-like structures, including ambiguous ones, 10 relatively large (>15 μm) solitary spheroids, and more than 10 film-like structures. Small spheroids are abundant and tend to occur as colony-like clusters. On the other hand, only 15 spindles, one lenticular structure, and a few spheroids were observed in WF6-1 and WF9-1. They appear to be far less well preserved than those contained in WF4-1.

Film-like structures in WF4-1 are granular to hyaline and are mostly single-sheeted, whereas some specimens appear to be branched. In either case, the structures are deformed to various degrees and are often associated with small spheroids or globules from 5 to 10 μm in diameter. Relatively small spheroidal structures tend to occur as clusters composed of more than 20 individuals that are associated with fluffy materials or film-like structures as described above (Fig. 9b–d). Spheroids larger than 15 μm occur solitarily, in most cases. The largest spheroid specimen is *ca.* 70 μm in diameter, has a hyaline wall, and contains some inner objects (Fig. 9e).

Sixty-one lenticular structures from WF4-1 range from 25 to 75 μm in the major dimension, but the majority are less than 50 μm. Many of the specimens appear to be filled with carbonaceous matter (Fig. 9f), although several specimens have hollow interiors. In the latter examples, continuous and hyaline walls can be identified (Fig. 9g). There are 65 spindle-like structures from WF4-1, and they range widely from 18 to 100 μm along the major dimension, but the majority are less than 50 μm. As a whole, the spindle-like structures from WF4-1 tend to be smaller compared with those from the

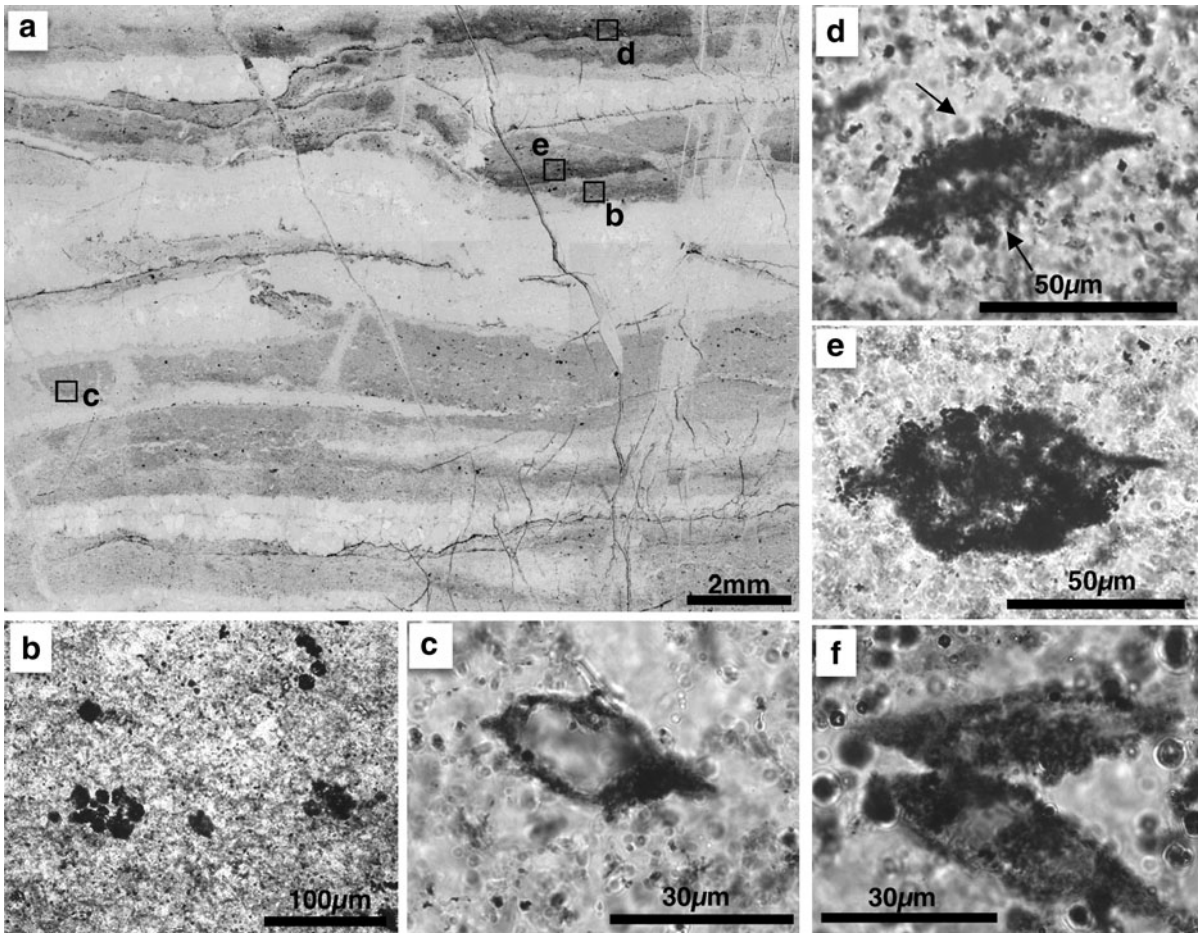

FIG. 10. Photomicrographs of bedded black chert from the Water Fall Ridge site and carbonaceous structures. (**a**) Composite photomicrograph of bedded black chert characterized by parallel lamination. The white layers are probably secondary cherts that fill bedding-parallel fractures. The squares show the positions of carbonaceous fossil-like structures shown in this figure. (**b**) Cluster of granular walled spheroids. Slide WF6-1, Position L-N57/1. (**c**) Hollow spindle with uneven appendage. Slide WF6-1, Position L-W61/4. (**d**) Poorly preserved spindle-like structure. The arrows show degraded portions of wall. Slide WF6-1, Position L-L54. (**e**) Highly granular spindle-like structure. Slide WF6-1, Position L-L57/1. (**f**) Obliquely paired degraded lenticular structures. Slide WF9-1, Position L-U47.

other sites. Whereas bodies of many lenses and spindles from the other sites are hollow and tend to be filled with pure chert, those from WF4-1 are enriched in carbonaceous matter inside and occasionally appear to be nearly solid (Fig. 9f, 9h). However, examination under intense transmitted light revealed that their interior is heterogeneous and translucent (Fig. 9i). Their superficial solid appearance can be attributed to the internal dense distribution of carbonaceous matter particles. Several specimens were found to have continuous and hyaline walls, which were, in some cases, deformed or partially broken (Fig. 9j, 9k). When appendages were clearly identified, they were generally of a flange type. Such lenticular to spindle-like structures occur as pairs or colony-like clusters, in addition to solitary occurrences. Parallel to obliquely arranged pairs of lenticular structures are common (Fig. 9l). Spindle-like structures rarely comprise linearly connected, paired, dumbbell-like structures, and colony-like clusters are also common. Clusters tend to be composed of 5–10 individuals and occasionally contain different morphologies (Fig. 9m, 9n): they are oriented either randomly or in parallel.

In WF6-1, spheroidal structures range 5–20 μm in diameter and occur as loose clusters (Fig. 10b). Their walls are highly granular, and detailed features are unknown. Lenticular and spindle-like structures from WF6-1 and WF9-1 range from 46 to 100 μm along the major dimension. They are hollow and have highly granular walls, blurred walls, or both (Fig. 10c–e). Although most of them occur solitarily, a few specimens composed of parallel to obliquely arranged pairs are present (Fig. 10f).

7. Syngeneity and Biogenicity of Microstructures

Sugitani *et al.* (2007, 2009a) discussed the origin of carbonaceous structures from the *ca.* 3000 Ma Farrel Quartzite of the Pilbara Craton, based on their syngeneity and biogenicity, using biogenicity criteria for Archean microfossils (Schopf and Walter, 1983; Buick, 1990; Westall and Folk, 2003; Hofmann, 2004; Brasier *et al.,* 2005). To confirm a microbial origin for the structures, six criteria were assessed, including (1) geological context and syngeneity, (2) composition, (3) morphological variation, (4) population and size distribution, (5) physical properties, and (6) elaboration in morphology and occurrence. Also in this study, these criteria are employed to assess the biogenicity of carbonaceous structures from the SPF. We discuss geological context, syngeneity, composition, and morphological variation of the structures of major morphological types together first. Biogenicity of each morphological type is then discussed based on population and size distribution, physical properties, and elaboration in morphology and occurrence.

7.1. Geological context

The geology and stratigraphy of all sampling sites have been well documented in previous and ongoing studies. The Archean age of the sedimentary successions from which the rock samples were collected has been fully demonstrated (Van Kranendonk, 1999, 2004a, 2004b; Smithies *et al.,* 2004; Hickman, 2008). In particular, at the Anchor Ridge and the Marble Bar Road sites, the age of deposition of host rocks are constrained directly by detrital zircons from underlying sandstones assigned to the Panorama Formation (Nelson, 1998, 2004) as well as other dated units (see Van Kranendonk *et al.,* 2007). The stratigraphic assignment of the Water Fall Ridge sedimentary succession to the SPF may be less convincing, due to limited age data (Hickman, 2008; Hickman, personal communication) and stratigraphic discontinuity between felsic volcaniclastic sandstone from which detrital zircons that gave an age of 3458 ± 9 Ma were obtained (Nelson, 2004) and the sedimentary succession from which samples for this study were collected (Fig. 8a). Nevertheless, for the following reasons we suggest that the Water Fall Ridge succession is the most likely correlative to the SPF. First, the succession has the same white and gray chert laminates (silicified carbonates) as most other places of the SPF in the Pilbara Craton, which is the defining characteristic of this formation. Second, the succession is unconformably overlain by greenish mafic volcaniclastic rocks assigned to the Euro Basalt. At the western Mount Grant, a similar mafic unit occurs and has unconformable upper and lower contacts. The upper unit is the *ca.* 3000 Ma fossil-bearing Farrel Quartzite that can be traced over 7 km along the strike from the type locality (Fig. 8a) (Sugitani *et al.,* 2007, 2009a, 2009b), whereas the lower unit is a sedimentary succession that includes white and gray chert laminite, evaporite, and sandstone, correlative to the Water Fall Ridge succession. So, available data are consistent with the sedimentary succession at the Water Fall Ridge being older than the Farrel Quartzite and attributable to the SPF.

The depositional environment of the SPF and origin of carbonaceous black chert in this formation have been controversial. Contrary to earlier studies (Lowe, 1983; Van Kranendonk *et al.,* 2003), Lindsay *et al.* (2005) suggested deposition in a hydrothermal setting and abiogenic hydrothermal origin of carbonaceous matter in black cherts, based on the discovery of a black chert vein system beneath a part of the SPF. However, it has subsequently been shown that the effects of hydrothermal alteration post-dated sediment deposition and were unrelated to the depositional setting of the protoliths to the SPF (Van Kranendonk, 2006). It is now generally considered that the SPF was most likely deposited in shallow-water marine and fluviatile environments (Allwood *et al.,* 2006, 2007; Van Kranendonk, 2006, 2007). For the Anchor Ridge site, a sedimentary origin of the black chert has been well documented through detailed sedimentological, stratigraphic, and geochemical studies (*e.g.,* Allwood *et al.,* 2006, 2007, 2010; Van Kranendonk, 2007). The stratigraphic and sedimentological studies presented here likewise indicate the sedimentary origin of the carbonaceous black cherts containing fossil-like structures at the Marble Bar Road and Waterfall Ridge sites. The black cherts occur as stratiform units in thick sedimentary successions of the SPF; are interbedded with sandstone, carbonate, evaporite, and volcaniclastic rocks; and are not associated with vein chert systems at these localities.

Hickman (2008) also suggested that cherts in the SPF are not primary in origin but exclusively represent wholly silicified carbonate sedimentary precursors. Whereas this is almost certainly the case for finely laminated white–light gray chert, and some examples of black chert (*e.g.,* Van Kranendonk, 2007), the lack of any evidence for silicification of carbonate rocks in the form of dispersed carbonate particles preclude this as a *de facto* conclusion for black cherts studied here. Furthermore, petrographic features of the black cherts

closely resemble those of primary carbonaceous black cherts of the Farrel Quartzite in the Goldsworthy greenstone belt (Sugitani *et al.,* 2007); thus we interpret carbonaceous cherts from the SPF to have been deposited primarily as chemically precipitated silica gel and diagenetically recrystallized to microcrystalline quartz.

7.2. Syngeneity

All carbonaceous structures occur in standard petrographic thin sections cut from fresh rock surfaces obtained from stratigraphically and lithologically controlled sections. They were commonly identified in duplicate sections. The structures cannot be post-metamorphic endolithic microbes, because carbonaceous particles are the same color as particles in the matrix, showing the same degree of thermal maturity. Syngeneity is not inconsistent with the presence of crosscutting veins (Fig. 9e, 9g, 9n) and the fact that they have been subjected to the same alteration events (*e.g.,* silicification and ferruginization) as their matrix. The structures occasionally comprise fine laminations together with carbonaceous particles disseminated in the matrix or thin layers a few millimeters or more in thickness (Fig. 6c), which suggests that they were once suspended and sedimented along with other detrital carbonaceous particles. These lines of evidence are consistent with syngeneity of the structures.

7.3. Composition

Raman spectra of selected specimens are shown in Fig. 11. Specimens from the Marble Bar Road site (Fig. 11a, 11d) and the Anchor Ridge site (Fig. 11b, 11c) show Raman spectra with an unresolved to poorly resolved G+D2 doublet centered at 1598–1606 cm^{-1}. Specimens from the Water Fall Ridge site (Fig. 11e–h) consistently show a G band centered at 1593–1598 cm^{-1} and distinct of its D2 shoulder at *ca.* 1612 cm^{-1}. All spectra show a small, flat shoulder near 1200 cm^{-1}, which indicates a D4 band as well as a poorly developed D3 band near 1500 cm^{-1}. All spectra show a D1 band at *ca.* 1345 cm^{-1} that varies, however, in relative intensity; spectra of specimens from the Marble Bar Road and the Anchor Ridge sites (Fig. 11a–d) show a D1/(G+D2) band height ratio varying between 1 and 1.28, whereas in the specimens from the Water Fall Ridge site (Fig. 11e–h) this

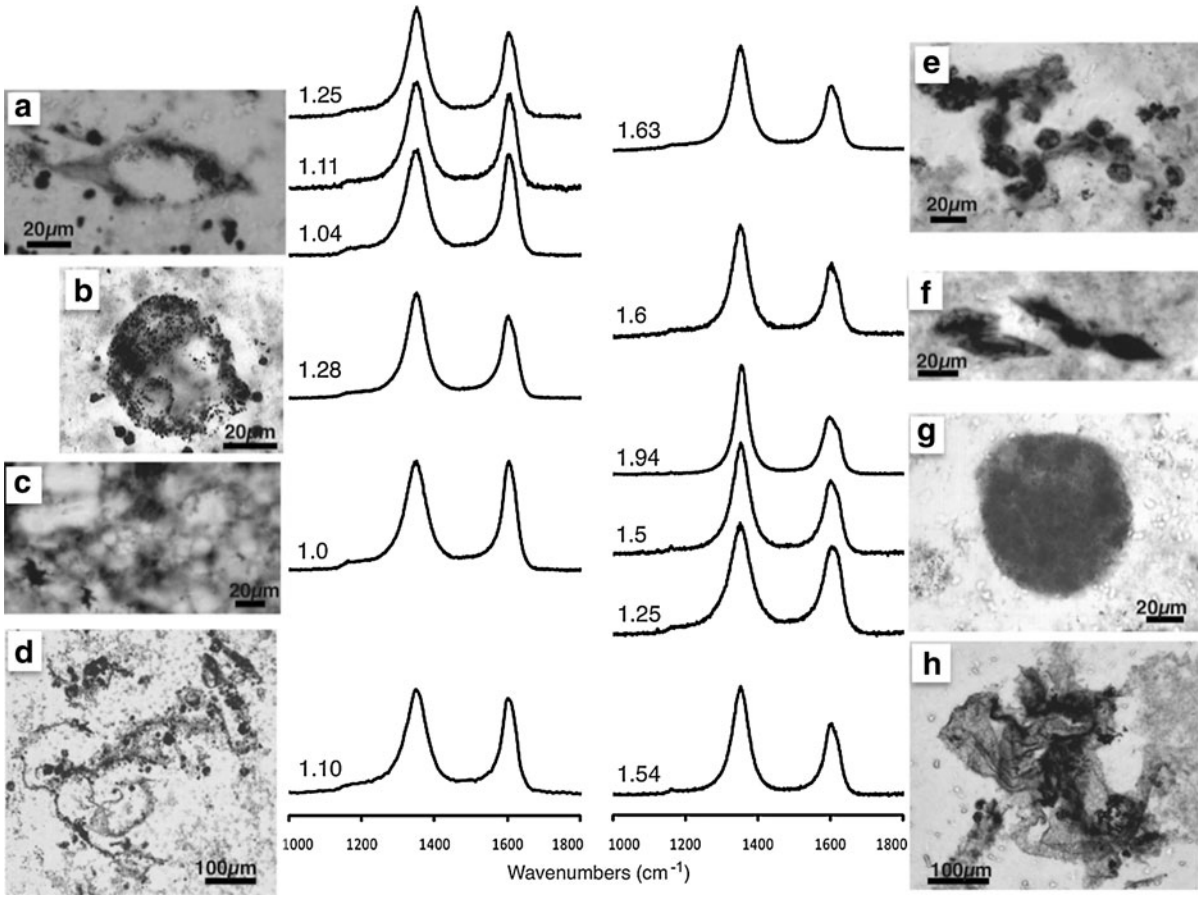

FIG. 11. Raman spectromicroscopy of carbonaceous microstructures. (**a**) Spindle-like structures showing micron-scale variation in Raman spectra. Slide MSC1-3d, Position L-K60. (**b**) Large spheroid. Slide TRD2a-6, Position L-C49. (**c**) Thread-like structures comprising a network pattern. Slide TRD2a-1, Position L-H43. (**d**) Film-like structure associated with spindle and spherical microstructures. Slide MSC1-3d, Position L-G62. (**e**) Small spheroids. Slide WF4-8, Position L-G51. (**f**) Lenticular structures. Slide WF4-8, Position L-M58. (**g**) Rounded carbonaceous clot showing micron-scale variations in Raman spectra. Slide WF4-8, Position L-O47. (**h**) Rippled film-like structures associated with several carbonaceous spheres. Slide WF4-8, L-H48. The height ratio of the two Raman bands (D1 and the G+D2 doublet) is given for each spectrum.

ratio varies between 1.25 and 1.94. Important differences in the relative intensity of the D1 band occur within fields several microns wide (Fig. 11a, 11g) and intermediate spectra with a D1/(G+D2) height ratio of *ca.* 1.25 occur in the two groups of samples. The height ratio R1 [=D1/G] and the area ratio R2 [=D1/(D1+G+D2)] were measured by fitting the D1-D4 and G bands with five Gauss-Lorentz bands (Beyssac *et al.*, 2002; Lepot *et al.*, 2008). A representative spectrum of the Marble Bar Road specimen (Fig. 11a, lower spectrum) has a R2 of 0.66 with a R1 of 1.19, whereas a representative spectrum of the Water Fall Ridge specimen (Fig. 11e) has a R2 of 0.68 with a R1 of 1.76.

Raman microspectroscopy demonstrated that the large and the small spheroidal structures, the lenticular to spindle-like structures, the threads, and the films are carbonaceous, although some differences in fine structure of spectra could be seen between specimens as described above (Fig. 11). The R1 ratio values higher than 1.0 and the R2 ratio of 0.66–0.68 indicate poorly organized carbonaceous matter that has been metamorphosed at most in the lower greenschist facies, at temperatures lower than 350°C, which is consistent to metamorphic grades assumed for fossil-like structures, as follows. The low intensity of the bands D3 and D4 and the distinct D2 band appearing as a shoulder in the specimen from the Water Fall Ridge site indicate a metamorphic overprint near the boundary between prehnite-pumpellyite and greenschist facies, which corresponds to peak temperatures of 300–350°C (Wopenka and Pasteris, 1993; Beyssac *et al.*, 2002). This is particularly clear for the Water Fall Ridge specimen that shows spectra similar to that of a black shale metamorphosed at *ca.* 330°C (Beyssac *et al.*, 2002). In most of the Raman spectra of the Marble Bar Road and the Anchor Ridge specimens, the D2 band cannot be clearly distinguished from the G band, which thus forms a doublet that is consequently shifted to higher wave numbers compared to the position of the G band in the Water Fall Ridge specimens. This indicates a higher contribution of the D2 band to the G+D2 doublet in samples of the Marble Bar Road and Anchor Ridge specimens. Since the D2 band progressively decreases in relative intensity with increasing thermal maturation, this indicates that the Water Fall Ridge specimens have been submitted to higher thermal alteration than samples of the first group. Furthermore, micron-scale heterogeneities in the Raman spectra of the carbonaceous matter were detected in specimens from the Marble Bar Road site (Fig. 11a) and from the Water Fall Ridge site (Fig. 11g). There is a continuum of the variation of the Raman spectra in those regions, which converge toward a similar spectrum for both groups of samples with intermediate values for the relative intensity of the D1 band. These heterogeneities may be explained by micron-scale differences in the chemistry of the organic precursor, different alteration pathways that lead to heterogeneities in the initiation of graphitization, or possibly orientation of the carbonaceous matter in the matrix (Beyssac *et al.*, 2003). The continuum in the variation of the spectra excludes the possibility of contamination of the rocks by metamorphosed carbonaceous particles. Moreover, the intermediate D1 intensity values common to the Water Fall Ridge specimens and the Marble Bar Road and Anchor Ridge specimens suggest that the difference in metamorphic overprint between these two groups is relatively low.

Table 1. Carbon Isotopic Values of Host Cherts

Sample	$\delta^{13}C_{PDB}$ (‰)
Trd2	−32.69
MSC1-1	−36.75
MSC1-2b	−35.65
MSC1-3	−32.60
WF-4	−31.01
WF-6	−36.07

Bulk carbon isotopic values of host cherts are shown in Table 1. Black cherts from the SPF range from −31.01‰ to −36.75‰, which are commonly characterized by lighter values than −30‰. The values are within the range of previously reported values of carbonaceous matter from Archean sedimentary rocks (*e.g.*, Hayes *et al.*, 1983). Bulk isotopic signatures and *in situ* Raman spectra are consistent with a microbial origin of carbonaceous matter of the microstructures in question.

7.4. Morphological variation

Five major morphological types—thread-like, film-like, spheroidal, lenticular, and spindle-like—were identified from the three sites assigned to the SPF. As described earlier, each morphological type includes subtypes. Spheroidal structures can be classified into small (<15 μm) and large (>15 μm) types. Small spheroids often occur as a colony-like cluster associated with film or fluffy materials. Some large spheroids have single spear- or blade-like appendages. Lenticular to spindle-like structures include a wide range of morphological types. Their bodies are either symmetrical or asymmetrical in shape. Appendages of spindle-like structures are commonly parallel to the major axis of the body, but their size and style of attachment to the body can vary. Such morphologically diverse structures occur together (for instance, Figs. 9a and 10a). This is contrastive to numerous possible gypsum ghosts in Fig. 6b that were undoubtedly formed by inorganic processes. On the other hand, Brasier *et al.* (2002, 2005) suggested that the morphological spectrum of microfossil-like structures in the ~3460 Ma Apex Chert (Schopf, 1993) can be explained by the redistribution of carbonaceous material during recrystallization of silica. The SPF black cherts were probably formed by recrystallization of silica gel as discussed above. Indeed, redistribution of carbonaceous matter occurred locally during recrystallization and formation of cavity-fill chert (Figs. 3e and 6c). However, morphologies of fossil-like carbonaceous structures discussed here are independent of crystal boundaries of matrix chert and spatially and morphologically unrelated to regions that exhibit redistribution textures of carbonaceous matter. The lack of spatial and morphological relationships with textures formed by redistribution of carbonaceous matter is consistent with the biogenicity of the carbonaceous structures.

7.5. Biogenicity assessment

As discussed above, geological context, syngeneity, composition, and morphological variation are consistent with the biogenicity of the SPF carbonaceous structures. In the fol-

lowing, the biogenicity of each morphological type is tested based on additional information, including population and size range, physical properties, and elaboration in morphology and occurrences.

7.5.1. Thread-like structures. Carbonaceous thread-like structures have often been reported from several localities of Archean volcanic-sedimentary successions, including volcanic glasses and vein chert, in addition to sedimentary chert layers (Awramik *et al* 1983; Walsh and Lowe, 1985; Rasmussen, 2000; Ueno *et al.,* 2001; Westall *et al.,* 2001; Kiyokawa *et al.,* 2006). They have been interpreted as fossilized chemotrophic or phototrophic prokaryotic microorganisms, although the biogenicity of such simple morphologies has often been controversial (Buick, 1984, 1988; Awramik *et al.,* 1988). Indeed, thread-like structures occur in colloform textured secondary cavity-fill chert of Archean age and have been interpreted as dubiofossils (Sugitani *et al.,* 2007).

While the carbonaceous thread-like structures from the Anchor Ridge site are also simple in morphology, their mode of occurrence favors interpretation that they are of "probable microbial origin." The thread-like structures are independent of the crystal boundaries of the matrix microcrystalline quartz and are assumed to have primarily comprised the network texture of the host chert, although in other places the texture is composed of broader and more ambiguous structures than those in Fig. 3c. The spectrum from thread to broader filamentous morphology may be attributed to bundling and degradation of thread-like structures.

Thread-like morphology is common for prokaryotic microorganisms. However, the network texture appears to merge horizontally or laterally into portions that show parallel lamination, where neither threads nor broader filaments can be clearly identified. Such occurrences seem inconsistent with the interpretation that the individual threads represent filamentous microorganisms. Rather, we suggest the possibility that this carbonaceous chert originated from an organic mat locally composed of fibrillar adhesive extracellular polymeric substances (EPS; Westall and Rincé, 1994; O'Toole *et al.,* 2000; Handley *et al.,* 2008). EPS can form three-dimensional fibrillar textures or films similar to those observed in this study and may act as templates for early silicification and lamina formation (Handley *et al.,* 2008). Pacton *et al.* (2007) proposed that such three-dimensional structures may survive lithification and advanced diagenesis. It has been suggested that alveolar organic structures observed in the silica- and clay-rich laminae of *ca.* 2700 Ma stromatolites may represent fossil EPS (Lepot *et al.,* 2009). Moreover, furan molecules detected in stromatolite-hosted *ca.* 2700 Ma kerogen (Sklarew and Nagy 1979) suggest the preservation of Archean carbohydrates, which are the main primary constituents of EPS. Very fine strands that interconnect to form a laminated web-like network similar to the SPF threads were observed in the *ca.* 3400 Ma Buck Reef Chert (Tice and Lowe, 2006). Thus, we suggest that carbonaceous threads could represent fossilized fibrils of biofilms, but not microorganisms.

7.5.2. Film-like structures. Supposed fossilized biofilms and biomats have been reported from Archean cherts by several authors. Well-preserved, abundant film-like structures are reported from the *ca* 3000 Ma Farrel Quartzite in the Goldsworthy greenstone belt (Sugitani *et al.,* 2007). They are interpreted as reworked and fragmented biofilms, communities of microorganisms composed of cells and mucous EPS. Westall *et al.* (2001, 2006) identified film-like structures on the HF-etched surface of Archean carbonaceous cherts from Western Australia and South Africa, and interpreted them as silicified biofilms. Carbonaceous laminations often found in thin sections that are cut perpendicular to the bedding plane of Archean cherts and sandstones are interpreted as biofilms (biomats) (Walsh, 1992; Noffke *et al.,* 2003, 2006, 2008; Tice and Lowe, 2004, 2006; Heubeck, 2009).

In the SPF, film-like structures composed of sheet-like arrangements of carbonaceous particles are abundant in the Water Fall Ridge site, whereas only three specimens have been identified from the Marble Bar Road site. No films were found in the Anchor Ridge site. All identified film-like structures appear to be folded or wrinkled, or both. The morphological variation is not related to boundaries of the matrix microcrystalline quartz, veins, secondary phase such as cavity-fill chert, or other minerals. Also, they do not show a spatial relationship with the host chert matrix, including flat deposition along well-defined bedding planes, as opposed to the laminae-associated threads.

Thus, the structures appear not to be a product of redistribution or condensation of organic matter during diagenesis and attending mineral formation. The morphological variation and the presence of notched edges (Fig. 7b, 7c) would suggest that they were composed of flexible but breakable material. As argued for film-like structures of the Farrel Quartzite (Sugitani *et al.,* 2007), films in the SPF potentially represent ripped-up clasts of microbial mats. Some of the structures are associated with small spheroids or globules (also discussed below). These attachments could be fossilized microbes interwoven within biofilms. The origin of simple films may need to be examined more cautiously, because formation by abiogenic process such as condensation of insoluble or soluble organic matter in the water column followed by sedimentation and polymerization into a kerogen or pyrobitumen precursor cannot be ruled out.

7.5.3. Spheroidal structures. Spheroidal structures are relatively common in the literature on Archean putative microfossils (*e.g* Knoll and Barghoorn, 1977; Dunlop *et al.,* 1978; Walsh, 1992; Westall *et al.,* 2001; Duck *et al.,* 2007; Sugitani *et al.,* 2007; Glikson *et al.,* 2008), although their biogenicity remains controversial (see Wacey, 2009, for instance). Skepticism about the biogenicity of carbonaceous spheroids is mostly due to their simple morphology, which is common also in abiogenic products, such as silica spherulite, sulfide, and carbonate (*e.g.,* Fox *et al.,* 1983; Brasier *et al.,* 2005). Particularly in the case of small spheroids, it is often unclear whether they are hollow or not, and detailed features of walls tend to be obscure. On the other hand, it has been suggested that dense cell-like structures may be preserved by polymerization of microbial cells (Lepot *et al.,* 2009) during diagenesis. Such dense cell-like organic globular structures were observed during experimental thermal degradation of modern cells (Glikson *et al.,* 2008), and their presence was suggested in 2700 Ma (Lepot *et al.,* 2009) and 3500 Ma (Glikson *et al.,* 2008) rocks. Thus, the fact that some spheroids are not hollow may not be a relevant abiogenicity criterion.

Even if they are hollow, their biogenicity could not be claimed without additional information such as colony-like occurrences, biological size range, taphonomic features, or obvious cell divisions (Sugitani *et al.,* 2007). Recent palynological and subsequent SEM and TEM studies indicate that the record of large (up to 300 μm) bona fide microfossils goes back to at least 3200 Ma (Grey and Sugitani, 2009; Javaux *et al.,* 2010).

Small spheroids. Small spheroids less than 15 μm in diameter were found in samples from the Marble Bar Road and the Water Fall Ridge sites. In the Marble Bar Road site, small spheroids tend to occur solitarily; only three colony-like clusters composed of approximately 15–40 spheroids were found. Most specimens from this site are poorly preserved (Fig. 7d), and their walls are highly granular and occasionally discontinuous. Some walls are extensively silicified and can be recognized only as traces. In either case, most of the spheroids are hollow. In the Water Fall Ridge site, more than 10 clusters of small spheroids occur in a single thin section of massive black chert, whereas in laminated to bedded chert, clearly identified spheroidal structures are not present. Some of the clusters are composed of more than 100 spheroids. Hyaline-walled hollow specimens are common. Additionally, an association of spheroid cluster with film-like structure or fluffy material is present (Fig. 9b, 9d). Although obvious abiogenic spherulitic structures such as colloform texture and dissolution cavities of sulfide spherules can be seen, they are distinct from carbonaceous spheroids. The small spheroids from the Water Fall Ridge site are likely biogenic and thus are regarded as probable microfossils. The biogenicity of small spheroids from the Marble Bar Road site is less convincing at this stage.

Large spheroids. The number of identified large spheroids from the SPF is limited (10 from the Anchor Ridge site, 1 from the Marble Bar Road site, 10 from the Water Fall Ridge site), and their size ranges widely from $\sim$15 μm up to 100 μm. While large spheroids with highly granular and dense walls (Fig. 4a) are more likely abiogenic, other specimens such as those shown in Fig. 7g and Fig. 9e are possibly biogenic. In these specimens, the walls appear to be hyaline, wrinkled, or partially broken, or both. This suggests that they were once composed of flexible but breakable material. Additionally, some specimens have inner objects. Such complexity and elaboration could discriminate them from coexisting abiogenic hollow structures formed by dissolution of pyrite aggregates and silica spherulites. It should be emphasized, however, that at this stage their biogenicity cannot be confirmed.

7.5.4. Lenticular to spindle-like structures. Lenticular to spindle-like structures in Archean cherts were first reported from the *ca* 3400 Ma Kromberg Formation in the Barberton greenstone belt, South Africa (Walsh, 1992), and recently from the *ca.* 3000 Ma Farrel Quartzite in the Goldsworthy greenstone belt (Fig. 8a).

Lenticular to spindle-like structures are abundant at all three sites discussed here. Thirty-eight specimens are present in a single thin section of black chert from the Anchor Ridge site, and 63 specimens occur in four thin sections from the Marble Bar Road site. Massive black chert from the Water Fall Ridge site contains numerous of these structures; more than 130 specimens are present in a single section. Size distribution of lenticular to spindle-like structures from the Anchor Ridge and the Marble Bar Road sites are nearly identical; most specimens range from 50 to 80 μm in the major dimension (Fig. 12a, 12b). Specimens in the massive chert from the Water Fall Ridge site, on the other hand, mostly range from 30 to 50 μm (Fig. 12c). In either case, the lenticular to spindle-like structures show a narrow size range (Fig. 12). These structures often occur as colony-like clusters or pairs, in which different morphological types are contained and individual objects can be oriented randomly. The random orientation and the colony-like distribution argue against a fenestral origin as suggested by Westall *et al.* (2001) on the basis of a distribution parallel to the sediment laminae.

Compared with large hollow spheroids and film-like structures, the lenticular to spindle-like structures tend to appear rigid. In addition, the Water Fall Ridge specimens appear to be solid and homogeneous. However, the appendage is occasionally curved (Fig. 4e), and the wall of the body can be wrinkled or partially broken (Fig. 4h and Fig. 9j, 9k). Examination using intense light revealed that "solid" appendage and body are actually heterogeneous and partially hollow (Figs. 4g and 9i). These features refute the possibility that they originated from fluid inclusions (Roedder, 1984; Dutkiewicz *et al.,* 1998). From these features, occurrences described above, and morphological complexity such as the flange-like appendages (Figs. 4j–l and 7m), the lenticular to spindle-like structures are considered probable microfossils.

8. Synthesis and Conclusion

The 3426–3350 Ma SPF (Hickman, 2008) is an Archean sedimentary succession widely identified in the East Pilbara Terrane of the Pilbara Craton (*e.g.,* Van Kranendonk *et al.,* 2006). This succession, which was deposited mainly in a shallow-water environment, has attracted interest because it contains stromatolites (*e.g.,* Allwood *et al.,* 2006; Van Kranendonk, 2007). The well-preserved and morphologically diverse stromatolites are thought to represent ecologically controlled architectures, although they are composed of recrystallized carbonate and bona fide microfossils have not yet been found within it or associated sedimentary rocks. In this study, we report morphologically diverse carbonaceous structures, including unusually large specimens up to 100 μm along the major dimension, from the three remote and widely separated localities assigned to the SPF, including the Panorama greenstone belt, the Warralong greenstone belt, and the Goldsworthy greenstone belt.

Five major morphological types were identified, including threads, films, spheroids, and lenticular and spindle-like structures. They are all syngenetic with their host sedimentary black chert. Their biogenicity was examined in the context of composition, populations, size variation, taphonomic features, and occurrences, the results of which suggest that film-like structures with small spheroids, cluster-forming small spheroids, and lenticular to spindle-like structures are probable microfossils. The biogenicity of large spheroids and simple films is less convincing at this stage. Mat-forming thread-like structures may represent fibrilar extracellular material.

Results of the present study are consistent with other reports of Archean large microfossils and possible microfossils

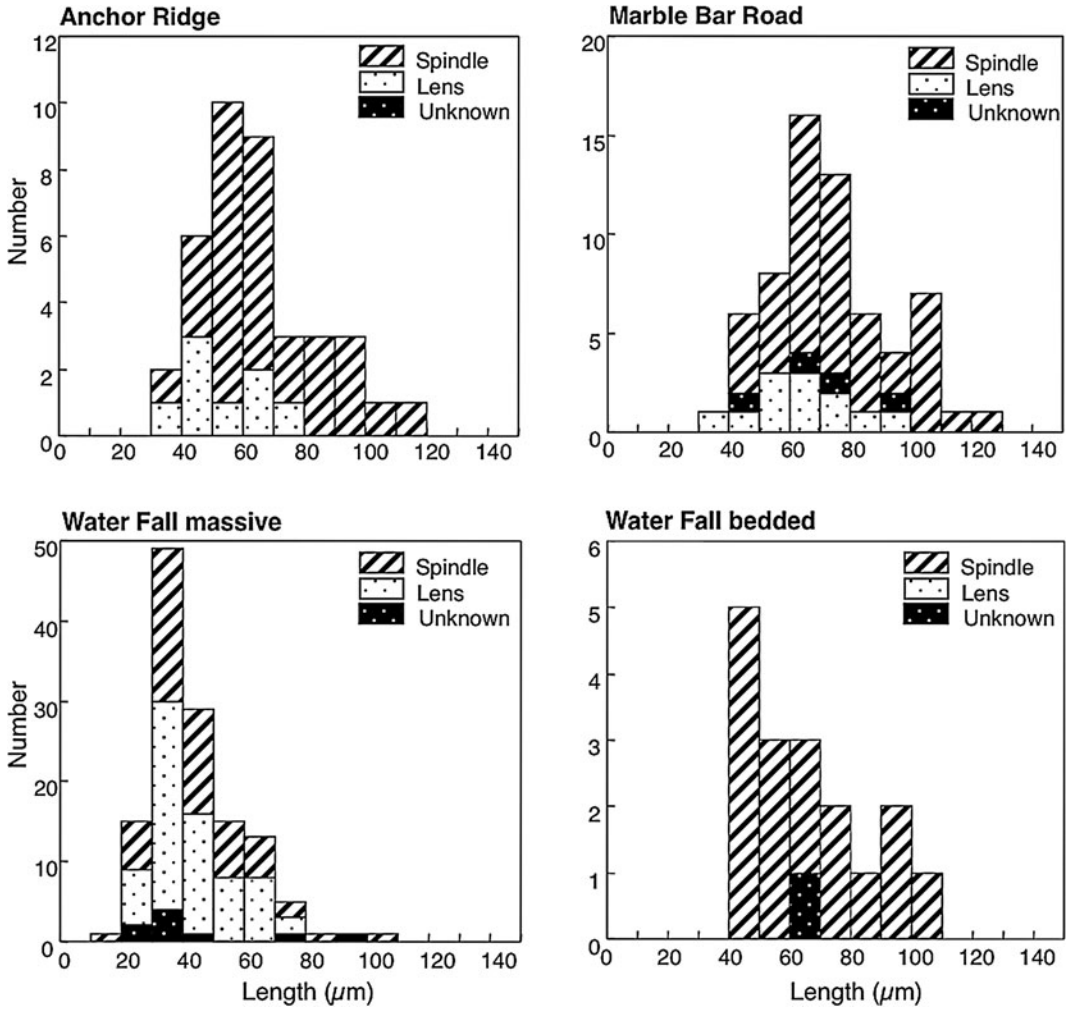

FIG. 12. Histograms for size (along the major axis) distributions of lenticular and spindle-like structures. Others show unclear structures that cannot be classified either into lenticular or spindle-like structures.

from the 3000 Ma Farrel Quartzite in the Pilbara Craton (*e.g.,* Sugitani *et al.,* 2007) and the 3200 Ma Moodies Group (Javaux *et al.,* 2010). Sugitani *et al.* (2007) reported carbonaceous microstructures of diverse morphologies (threads, films, spheroids, and lens-spindles) from the Archean sedimentary succession of the *ca.* 3000 Ma Farrel Quartzite of the Gorge Creek Group, at the Goldsworthy greenstone belt in the Pilbara Craton, Western Australia. Their biogenicity was inferred from indigenousness, syngeneity, sedimentary origin of the host chert, abundant population, narrow size distribution, carbonaceous composition, evidence of flexible or breakable walls, apparent taphonomic features, and the presence of colony-like aggregations. This was supported by the fact that the structures are organic-walled and can be extracted by palynological procedures (Grey and Sugitani, 2009) and that the structures are enriched in nitrogen and sulfur as well as carbon (Oehler *et al.,* 2009, 2010). A systematic rare-earth element and yttrium study showed that the host carbonaceous cherts were deposited in a moderate and habitable environment but not in a high-temperature hydrothermal environment (Sugahara *et al.,* 2010). Sugitani *et al.* (2009b) also reconstructed three-dimensional images of selected specimens and demonstrated the three-dimensionally preserved complex morphologies represented by a flange-like appendage, which provided further evidence for the biogenicity of the Farrel Quartzite assemblage. The biogenicity of the *ca.* 3000 Ma Farrel Quartzite assemblage, including large microfossils up to 100 μm, seems to be established. More recently Javaux *et al.* (2010) reported large (up to 300 μm) spheroidal organic-walled carbonaceous structures from the 3200 Ma Moodies Group, the Barberton greenstone belt. Preserved cellular ultra-structures in addition to syngeneity, carbonaceous composition, populations, size range, and taphonomic features are convincing lines of evidence for their biogenicity. Continuous cellular structures encapsulated or filled by minerals, or both, support a microfossil origin, as opposed to intermineral organic matter filling voids (*e.g.,* triple junctions) at grain boundaries (Lepot *et al.,* 2009). These studies argue for a biogenic origin for the large and diverse carbonaceous microstructures observed in early to mid-Archean sedimentary successions and that they could include fossil cells, sheaths, and EPS.

Compared with these cases, the study of the SPF structures is at the preliminary stage, and further investigations including palynology and nanoscale chemical analyses are required to independently establish their biogenicity.

However, the microbial origin of the SPF structures is very promising. Finally, it may be noted again that spheroidal and spindle-like carbonaceous structures, similar to or even larger in size than the SPF structures, were previously reported from the *ca.* 3400 Ma Kromberg Formation in the Barberton greenstone belt, South Africa, almost contemporaneous with the SPF (Walsh, 1992). Occurrences of similar spindle-like structures from the Farrel Quartzite, the SPF, and the Kromberg Formation are of special interest, considering their complex morphologies that are generally unexpected for Archean microfossils. Further and comprehensive studies should be required to reveal their significance in the early evolution of life.

Acknowledgments

Financial support to K.S. from the Japan Society for the Promotion of Science (the Joint Research Program, Japan-Australia and a grant-in-aid, No. 19340150) and from the FNRS (Belgium National Funds for Research postdoctoral fellowship) to K.L. are gratefully acknowledged. Helpful comments and encouragement by Kath Grey and Emmanuelle Javaux are greatly appreciated. We also appreciate Arthur Hickman, who provided useful comments on the stratigraphic interpretations on the SPF. Maud Walsh and an anonymous referee are acknowledged for their constructive comments. We thank Sherry Cady for her editorial assistance. Raman analyses were funded by a FRFC No. 2.4.558.09 grant (E.J.) and Region Ile-de-France (IPG Paris).

Abbreviations

EPS, extracellular polymeric substances; SPF, Strelley Pool Formation.

References

Allwood, A.C., Walter, M.R., Kamber, B.S., Marshall, C.P., and Burch, I.W. (2006) Stromatolite reef from the Early Archaean era of Australia. *Nature* 441:714–718.

Allwood, A.C., Burch, I., and Walter, M.R. (2007) Stratigraphy and facies of the 3.43 Ga Strelley Pool Chert in the southwestern North Pole Dome, Pilbara Craton, Western Australia. *Geological Survey of Western Australia, Record 2007/11,* Geological Survey of Western Australia, East Perth.

Allwood, A.C., Kamber, B.S., Walter, M.R., Burch, I.W., and Kanik, I. (2010) Trace elements record depositional history of an Early Archean stromatolitic carbonate platform. *Chem Geol* 270:148–163.

Awramik, S.M., Schopf, J.W., and Walter, M.R. (1983) Filamentous fossil bacteria from the Archean of Western Australia. *Precambrian Res* 20:357–374.

Awramik, S.M., Schopf, J.W., and Walter, M.R. (1988) Carbonaceous filaments from the North Pole, Western Australia: are they fossil bacteria in Archean stromatolites? A discussion. *Precambrian Res* 39:303–309.

Beyssac, O., Goffé, B., Chopin, C., and Rouzaud, J.-N. (2002) Raman spectra of carbonaceous material in metasediments: a new geothermometer. *Journal of Metamorphic Geology* 20:859–871.

Beyssac, O., Goffé, B., Petitet, J.-P., Froigneux, E., Moreau, M., and Rouzaud, J.-N. (2003) On the characterization of disordered and heterogeneous carbonaceous materials by Raman spectroscopy. *Spectrochim Acta A Mol Biomol Spectrosc* 59:2267–2276.

Brasier, M.D., Green, O.R., Jephcoat, A.P., Kleppe, A.K., Van Kranendonk, M.J., Lindsay, J.F., Steele, A., and Grassineau, N.V. (2002) Questioning the evidence for Earth's oldest fossils. *Nature* 416:76–81.

Brasier, M.D., Green, O.R., Lindsay, J.F., McLoughlin, N., Steele, A., and Stoakes, C. (2005) Critical testing of Earth's oldest putative fossil assemblage from the ~3.5 Ga Apex chert, Chinaman Creek, Western Australia. *Precambrian Res* 140: 55–102.

Brasier, M., McLoughlin, N., Green, O., and Wacey, D. (2006) A fresh look at the fossil evidence for early Archaean cellular life. *Philos Trans R Soc Lond B Biol Sci* 361:887–902.

Buick, R. (1984) Carbonaceous filaments from North Pole, Western Australia: are they fossil bacteria in Archaean stromatolites? *Precambrian Res* 24:157–172.

Buick, R. (1988) Carbonaceous filaments from North Pole, Western Australia: are they fossil bacteria in Archaean stromatolites? A reply. *Precambrian Res* 39:311–317.

Buick, R. (1990) Microfossil recognition in Archean rocks; an appraisal of spheroids and filaments from a 3500 m.y. old chert-barite unit at North Pole, Western Australia. *Palaios* 5:441–459.

DiMarco, M.J. and Lowe, D.R. (1989) Stratigraphy and sedimentology of an early Archean felsic volcaniclastic sequence, eastern Pilbara Block, Western Australia, with special reference to the Duffer Formation and implications for crustal evolution. *Precambrian Res* 44:147–169.

Duck, L.J., Glikson, M., Golding, S.D., and Webb, R.E. (2007) Microbial remains and other carbonaceous forms from the 3.24 Ga Sulphur Springs black smoker deposit, Western Australia. *Precambrian Res* 154:205–220.

Dunlop, J.S.R., Milne, V.A., Groves, D.I., and Muir, M.D. (1978) A new microfossil assemblage from the Archaean of Western Australia. *Nature* 274:676–678.

Dutkiewicz, A., Rasmussen, B., and Buick, R. (1998) Oil preserved in fluid inclusions in Archaean sandstones. *Nature* 395:885–888.

Fox, S.W., Syren, R.M., Ingram, M., Price, B.J., and Costello, J. (1983) Ancient microspheres: abiogenic, proterobiogenic, or biogenic? *Precambrian Res* 23:1–8.

Glikson, M., Duck, L.J., Golding, S.D., Hofmann, A., Bolhar, R., Webb, R., Baiano, J.C.F., and Sly, L.I. (2008) Micorbial remains in some earliest Earth rocks: comparison with a potential modern analogue. *Precambrian Res* 164:187–200.

Grey, K. and Sugitani, K. (2009) Palynology of Archean microfossils (c. 3.0 Ga) from the Mount Grant area, Pilbara Craton, Western Australia: further evidence of biogenicity. *Precambrian Res* 173:60–69.

Grotzinger, J.P. and Knoll, A.H. (1999) Stromatolites in Precambrian carbonates: evolutionary mileposts or environmental dipsticks? *Annu Rev Earth Planet Sci* 27:313–358.

Grotzinger, J.P. and Rothman, D.H. (1996) An abiotic model for stromatolite morphogenesis. *Nature* 383:423–425.

Handley, K.M., Turner, S.J., Campbell, K.A., and Mountain, B.W. (2008) Silicifying biofilm exopolymers on a hot-spring microstromatolite: templating nanometer-thick laminae. *Astrobiology* 8:747–770.

Hayes, J.M., Kaplan, I.R., and Wedeking, K.W. (1983) Precambrian organic geochemistry, preservation of the record. In *Earth's Earliest Biosphere: Its Origin and Evolution*, edited by J.W. Schopf, Princeton University Press, Princeton, pp 93–134.

Heubeck, C. (2009) An early ecosystem of Archean tidal microbial mats (Moodies Group, South Africa, *ca.* 3.2 Ga). *Geology* 37:931–934.

Hickman, A.H. (2008) Regional review of the 3426–3350 Ma Strelley Pool Formation, Pilbara Craton, Western Australia. *Geological Survey of Western Australia, Record 2008/15,* Geological Survey of Western Australia, East Perth.

Hofmann, H.J. (2004) Archean microfossils and abiomorphs. *Astrobiology* 4:135–136.

Hofmann, H.J., Grey, K., Hickman, A.H., and Thorpe, R.I. (1999) Origin of 3.45 Ga coniform stromatolites in Warrawoona Group, Western Australia. *Geol Soc Am Bull* 111:1256–1262.

Javaux, E.J., Marshall, C.P., and Bekker, A. (2010) Organic-walled microfossils in 3.2-billion-year-old shallow-marine siliciclastic deposits. *Nature* 463:934–938.

Kiyokawa, S., Ito, T., Ikehara, M., and Kitajima, F. (2006) Middle Archean volcano-hydrothermal sequence: bacterial microfossil-bearing 3.2 Ga Dixon Island Formation, coastal Pilbara terrane, Australia. *Geol Soc Am Bull* 118:3–22.

Knoll, A.H. and Barghoorn, E.S. (1977) Archean microfossils showing cell division from the Swaziland system of South Africa. *Science* 198:396–398.

Lepot, K., Benzerara, K., Brown, G.E., Jr, and Philippot, P. (2008) Microbially influenced formation of 2,724-million-year-old stromatolites. *Nat Geosci* 1:118–121.

Lepot, K., Benzerara, K., Rividi, N., Cotte, M., Brown, G.E., Jr, and Philippot, P. (2009) Organic matter heterogeneities in 2.72 Ga stromatolites: alteration versus preservation by sulphur incorporation. *Geochim Cosmochim Acta* 73:6579–6599.

Lindsay, J.F., Brasier, M.D., McLoughlin, N., Green, O.R., Fogel, M., Steele, A., and Mertzman, S.A. (2005) The problem of deep carbon—an Archean paradox. *Precambrian Res* 143:1–22.

Lowe, D.R. (1980) Stromatolites 3,400-Myr old from the Archean of Western Australia. *Nature* 284:441–443.

Lowe, D.R. (1983) Restricted shallow-water sedimentation of Early Archean stromatolitic and evaporitic strata of the Strelley Pool Chert, Pilbara Block, Western Australia. *Precambrian Res* 19:239–283.

Lowe, D.R. (1994) Abiological origin of described stromatolite older than 3.2 Ga. *Geology* 22:387–390.

Marshall, C.P., Love, G.D., Snape, C.E., Hill, A.C., Allwood, A.C., Walter, M.R., Van Kranendonk, M.J., Bowden, S.A., Sylva, S.P., and Summons, R.E. (2007) Structural characterization of kerogen in 3.4 Ga Archaean cherts from the Pilbara Craton, Western Australia. *Precambrian Res* 155:1–23.

McCollom, T.M. and Seewald, J.S. (2006) Carbon isotope composition of organic compounds produced by abiotic synthesis under hydrothermal conditions. *Earth Planet Sci Lett* 243:74–84.

McLoughlin, N., Wilson, L.A., and Brasier, M.D. (2008) Growth of synthetic stromatolites and wrinkle structures in the absence of microbes—implications for the early fossil record. *Geobiology* 6:95–105.

Nelson, D.R. (1998) 142836: volcaniclastic sedimentary rock, Gorge Creek; Geochronology dataset 393. In *Compilation of Geochronology Information, 2009 Update,* Geological Survey of Western Australia, East Perth.

Nelson, D.R. (2004) 169026: volcaniclastic metasandstone, Lawson Well; Geochronology dataset 61. In *Compilation of Geochronology Data, June 2006 Update,* Geological Survey of Western Australia, East Perth.

Noffke, N., Hazen, R., and Nhelko, N. (2003) Earth's earliest microbial mats in a siliciclastic marine environment (2.9 Ga Mozaan Group, South Africa). *Geology* 31:673–676.

Noffke, N., Eriksson, K.A., Hazen, R.M., and Simpson, E.L. (2006). A new window into Early Archean life: microbial mats in Earth's oldest siliciclatic tidal deposits (3.2 Ga Moodies Group, South Africa). *Geology* 34:253–256.

Noffke, N., Beukes, N., Bower, D., Hazen, R.M., and Swift D.J.P. (2008) An actualistic perspective into Archean worlds—(cyano-)bacterially induced sedimentary structures in the siliciclastic Nhlazatse Section, 2.9 Ga Pongola Supergroup, South Africa. *Geobiology* 6:5–20.

Oehler, D.Z., Robert, F., Walter, M.R., Sugitani, K., Allwood, A., Meibom, A., Mostefaoui, S., Selo, M., Thomen, A., and Gibson, E.K. (2009) NanoSIMS: insights to biogenicity and syngeneity of Archaean carbonaceous structures. *Precambrian Res* 173:70–78.

Oehler, D.Z., Robert, F., Walter, M.R., Sugitani, K., Meibom, A., Mostefaoui, S., and Gibson, E.K. (2010) Diversity in the Archaean biosphere: new insights from NanoSIMS. *Astrobiology* 10:413–424.

O'Toole, G., Kaplan, H.B., and Kolter, R. (2000) Biofilm formation as microbial development. *Annu Rev Microbiol* 54:49–79.

Pacton, M., Fiet, N., and Gorin, G. (2007) Bacterial activity and preservation of sedimentary organic matter: the role of exopolymeric substances. *Geomicrobiol J* 24:571–581.

Rasmussen, B. (2000) Filamentous microfossils in a 3,235-million-year-old volcanogenic massive sulphide deposit. *Nature* 405: 676–679.

Roedder, E. (1984) Fluid inclusions. *Reviews in Mineralogy* 12: 59–77.

Schopf, J.W. (1993) Microfossils of the Early Archean Apex chert: new evidence of the antiquity of life. *Science* 260:640–646.

Schopf, J.W. and Walter, M.R. (1983) Archean microfossils: new evidence of ancient microbes. In *Earth's Earliest Biosphere, Its Origin and Evolution,* edited by J.W. Schopf, Princeton University Press, Princeton, pp 214–239.

Sklarew, D.S. and Nagy, B. (1979) 2,5-Dimethylfuran from $\sim 2.7 \times 10^9$-year-old Rupemba-Belingwe stromatolite, Rhodesia: potential evidence for remnants of carbohydrates. *Proc Natl Acad Sci USA* 76:10–14.

Smithies, R.H., Van Kranendonk, M.J., and Hickman, A.H. (2004) De Grey, W.A. Sheet 2757 (Version 2.0): Western Australia Geological Survey, 1:100 000 Geological Series.

Sugahara, H., Sugitani, K., Mimura, K., Yamashita, F., and Yamamoto, K. (2010) A systematic rare-earth elements and yttrium study of Archean cherts at the Mount Goldsworthy greenstone belt in the Pilbara Craton: implications for the origin of microfossil-bearing black cherts. *Precambrian Res* 177:73–87.

Sugitani, K., Grey, K., Allwood, A., Nagaoka, T., Mimura, K., Minami, M., Marshall, C.P., Van Kranendonk, M.J., and Walter, M.R. (2007). Diverse microstructures from Archaean chert from the Mount Goldsworthy–Mount Grant area, Pilbara Craton, Western Australia: microfossils, dubiofossils, or pseudofossils? *Precambrian Res* 158:228–262.

Sugitani, K., Grey, K., Nagaoka, T., Mimura, K., and Walter, M.R. (2009a) Taxonomy and biogenicity of Archaean spheroidal microfossils (*ca.* 3.0 Ga) from the Mount Goldsworthy–Mount Grant area in the northeastern Pilbara Craton, Western Australia. *Precambrian Res* 173:50–59.

Sugitani, K., Grey, K., Nagaoka, T., and Mimura, K. (2009b) Three-dimensional morphological and textural complexity of Archean putative microfossils from the northeastern Pilbara Craton: indications of biogenicity of large ($>15\ \mu$m) spheroidal and spindle-like structures. *Astrobiology* 9:603–615.

Tice, M.M. and Lowe, D.R. (2004). Photosynthetic microbial mats in the 3,416-Myr-old-ocean. *Nature* 431:549–552.

Tice, M.M. and Lowe, D.R. (2006). The origin of carbonaceous matter in pre-3.0 Ga greenstone terrains: a review and new evidence from the 3.42 Ga Buck Reef Chert. *Earth-Science Reviews* 76:259–300.

Ueno, Y., Isozaki, Y., Yurimoto, H., and Maruyama, S. (2001) Carbon isotopic signatures of individual Archean microfossils (?) from Western Australia. *Int Geol Rev* 43:196–212.

Van Kranendonk, M.J. (1999) North Shaw, W.A. Sheet 2755: Western Australia Geological Survey, 1:100 000 Geological Series.

Van Kranendonk, M.J. (2004a) Carlindie, W.A. Sheet 2756: Western Australia Geological Survey, 1:100 000 Geological Series.

Van Kranendonk, M.J. (2004b) Coongan, W.A. Sheet 2856: Western Australia Geological Survey, 1:100 000 Geological Series.

Van Kranendonk, M.J. (2006) Volcanic degassing, hydrothermal circulation and the flourishing of early life on Earth: a review of the evidence from c. 3490–3240 Ma rocks of the Pilbara Supergroup, Pilbara Craton, Western Australia. *Earth-Science Reviews* 74:197–240.

Van Kranendonk, M.J. (2007) A review of the evidence for putative Paleoarchean life in the Pilbara Craton. In *Earth's Oldest Rocks,* Developments in Precambrian Geology 15, edited by M.J. Van Kranendonk, R.H. Smithies, and V. Bennet, Elsevier, Amsterdam, pp 855–896.

Van Kranendonk, M.J., Webb, G.E., and Kamber, B.S. (2003) Geological and trace element evidence for a marine sedimentary environment of deposition and biogenicity of 3.45 Ga stromatolitic carbonates in the Pilbara Craton, and support for a reducing Archaean ocean. *Geobiology* 1:91–108.

Van Kranendonk, M.J., Smithies, R.H., Hickman, A.H., Bagas, L., Williams, I.R., and Farrell, T.R. (2004) Event stratigraphy applied to 700 million years of Archaean crustal evolution, Pilbara Craton, Western Australia. In *Geological Survey of Western Australia Annual Review 2003-04,* Geological Survey of Western Australia, East Perth.

Van Kranendonk, M.J., Hickman, A.H., Smithies, R.H., Williams, I.R., Bagas, L., and Farrell, T.R. (2006) Revised lithostratigraphy of Archean supracrustal and intrusive rocks in the northern Pilbara Craton, Western Australia. *Western Australia Geological Survey, Record 2006/15,* Geological Survey of Western Australia, East Perth.

Van Kranendonk, M.J., Smithies, R.H., Hickman, A.H., and Champion, D.C. (2007) Review: secular tectonic evolution of Archean continental crust: interplay between horizontal and vertical processes in the formation of the Pilbara Craton, Australia. *Terra Nova* 19:1–38.

Van Kranendonk, M.J., Smithies, R.H., Hickman, A.H., Wingate, M.T.D., and Bodorkos, S. (2010) Evidence for Mesoarchean (~3.2 Ga) rifting of the Pilbara Craton: the missing link in an early Precambrian Wilson cycle. *Precambrian Res* 177:145–161.

Wacey, D. (2009) *Early Life on Earth: A Practical Guide,* Springer, Heidelberg.

Walsh, M.M. (1992) Microfossils and possible microfossils from Early Archean Onverwacht Group, Barberton Mountain Land, South Africa. *Precambrian Res* 54:271–293.

Walsh, M.M. and Lowe, D.R. (1985) Filamentous microfossils from the 3,500-Myr-old Onverwacht Group, Barberton Mountain Land, South Africa. *Nature* 314:530–532.

Westall, F. and Folk, R.L. (2003) Exogenous carbonaceous microstructures in Early Archeaen cherts and BIFs from the Isua Greenstone belt: implications for the search for life in ancient rocks. *Precambrian Res* 126:313–330.

Westall, F. and Rincé, Y. (1994) Biofilms, microbial mats and microbe-particle interactions: electron microscope observations from diatomaceous sediments. *Sedimentology* 41:147–162.

Westall, F., de Wit, M.J., Dann, J., van der Gaast, S., de Ronde, C.E.J., and Gerneke, D. (2001) Early Archean fossil bacteria and biofilms in hydrothermally-influenced sediments from the Barberton greenstone belt, South Africa. *Precambrian Res* 106:93–116.

Westall, F., de Vries, S.T., Nijman, W., Rouchon, V., Orberger, B., Pearson, V., Watson, J., Verchovsky, A., Wright, I., Rouzaud, J.-N., Marchesini, D., and Severine, A. (2006) The 3.446 Ga "Kitty's Gap Chert," an early Archean microbial ecosystem. *Geological Society of America Special Papers* 405:105–131.

Wopenka, B. and Pasteris, J.D. (1993) Structural characterization of kerogens to granulite-facies graphite: applicability of Raman microprobe spectroscopy. *American Mineralogist* 78:533–557.

Address correspondence to:
Kenichiro Sugitani
Department of Environmental Engineering and Architecture
Graduate School of Environmental Studies
Nagoya University
Nagoya 464-8601
Japan

E-mail: sugi@info.human.nagoya-u.ac.jp

Submitted 13 September 2010
Accepted 16 October 2010